AD NUMBER
AD003742
CLASSIFICATION CHANGES
TO: unclassified
FROM: restricted
LIMITATION CHANGES
TO: Approved for public release, distribution unlimited
FROM: Distribution authorized to U.S. Gov't. agencies and their contractors; Administrative/Operational Use; FEB 1953. Other requests shall be referred to Office of Naval Research, Arlington, VA 22217.
AUTHORITY
E.O. 10501 dtd 5 Nov 1953; Office of Naval Research ltr dtd 9 Nov 1977

~~80~~ NO 3742 CLASSIFICATION

DSC-PP11 Camera Unit

Strip into Original Film

Reproduce one copy to forward to DSC-SD11 (Mr. Hinshaw)

Reproduce one copy to forward to DSC-SD11 (Miss Grant)

Forward Original copy to DSC-PRC (Mr. Pilgrim)

Reproduce two copies for Mary Potter to send to Washington.

19 March 1953

Memorandum to Distribution List, Contract Nonr-22215.

The recent technical report "Wave Transformation: Preliminary Report" issued in February, 1953 should be Series 29, Issue 54 rather than Series 29, Issue 53 as shown on the cover and on the title page.

Waves Research Laboratory
University of California
Berkeley 4, California

UNIVERSITY OF CALIFORNIA
INSTITUTE OF ENGINEERING RESEARCH
BERKELEY 4, CALIFORNIA

WAVE TRANSFORMATION: PRELIMINARY REPORT

by

R. L. Wiegel, O. Sibul, M. Hall, R. A. Fuchs,
E. S. O'Keefe, J. R. Morison, and R. R. Putz

SERIES NO. 29
ISSUE NO. 53
DATE February, 1953

63

University of California
Department of Engineering
Submitted under Contract Nonr-222(15)
with the Office of Naval Research (NR-256-001)

Institute of Engineering Research
Waves Research Laboratory
Technical Report
Series 29, Issue 53

Wave Transformation: Preliminary Report

by

R. L. Wiegel, O. Sibul, M. Hall, R.A. Fuchs,
E.S. O'Keefe, J.R. Morison, and R. R. Putz

Berkeley, California
February 1953

TABLE OF CONTENTS

Study of Relationships of Swell and Breaker Characteristics and the Transformation of Waves in Shoaling Water

Contract Nonr-222(15), Project NR 266-001

Wave Transformation: Preliminary Report
Series 29, Issue 54
January 1953

A. INTRODUCTION

Winds blowing over the ocean generate waves on the water surface which are as variable as the winds which create them. They vary in height, length, and breadth. Within the storm area they are known as wind waves and often appear as irregular mounds (Figure 1). After leaving the storm area they decrease in height and increase in length and breadth due to dispersion, air resistance, viscosity, turbulence, etc. They transform into swell, and eventually they may enter shoaling water along coasts, finally breaking over reefs, against cliffs, and along beaches.

If, during an amphibious landing, the variation in breaker heights could be predicted, a mechanism would be available by which landing craft could be directed through the surf during intervals of relatively low breakers. It was thought that a possible method for the prediction of relatively calm surf might be formulated from a study of the relation between off-shore swells and the breakers on a beach. If such a relationship could be established, readings from wave recorders operating aboard off-shore ships could be used during days of high surf to direct landing craft so that their arrival time would coincide with the intermittent intervals of relatively low surf.

Preliminary studies indicated that the general problem was extremely complex due to the dispersive, short-crested, and refractive properties of waves. These properties are discussed briefly below:

Dispersion: Wave velocity in deep water depends primarily upon wave length, and to a small extent upon wave height; in shoaling water wave velocity depends upon wave length and water depth, as well as to a small extent upon wave height. The more shallow the water the greater is the effect of depth and the less is the effect of wave length upon wave velocity. As long as the velocity is dependent upon wave length it is said to be dispersive.

Consider a typical record such as the one shown in Figure 2. It can be seen that both the heights and the intervals between successive crests (hence, lengths) vary. Because of this variability it can be shown in a rather simple manner that the "waves" cannot be of permanent form. For if they were, then the crests would be moving with velocities associated with the lengths and as the successive lengths vary, the velocities would vary; hence, the spaces between crests would change. It follows, then, that they cannot be of permanent form. In fact, observations of waves in the generating area have indicated that the crests cannot be followed for more than a few wave lengths: old crests gradually disappear and new crests appear (See Figure 7). It would seem reasonable that the distance through which

individual crests could be followed would depend upon the width of the frequency spectrum. Hence, the first long swells arriving from a distant storm, consisting of waves of nearly the same frequency, probably could be tracked for a considerably greater distance than the waves in the generating area (an observed fact). The average condition would, of course, lie between these two limits.

In the general case, then, instead of following individual crests, or groups, from one location to another and merely determining the travel time, one must treat the transformation in both space and time of a so-called "colored noise" random time series. In order to develop the relationship between the disturbance of the ocean surface as it exists offshore and the breakers along a beach it is necessary to utilize Fourier Series, Fourier Integrals or random function analyses of the surface fluctuations combined with the linear wave theory.

Fortunately, the dependency of wave velocity on wave length decreases as the water depth decreases. In fact, on a beach the velocity of a wave as it breaks is nearly independent of length; it depends almost entirely upon the water depth. Thus, an observer on a pier watching relatively long swells travel from the end of the pier to the breaker zone, can easily follow the individual crests. Because of this relative insensitivity near shore it is felt that a relatively simple solution may be obtainable for many cases.

Short-crestedness (See Figure 3): Consider the case of a wave recorder being located as is shown in Figure 4. Because the waves are short-crested, the height of the breakers can be directly predicted only along a relatively short section of the beach. At other locations the breaker heights may be higher or lower. For beaches of small length this will not be as important as for long beaches.

Observations indicate that the crest-length (i.e., breadth) depends largely upon the distance the waves have travelled from the storm area; the greater the distance the longer the crest-length. Hence, swell from distant storms should present less a problem than local waves.

Refraction: When waves enter water in which the depth is less than half their length their velocity depends upon the depth as well as their length, so waves travelling at an angle to the underwater contours will bend (Figure 4). Because of this it is not possible to predict directly the effect of wave transformation along a line parallel to their direction of travel in deep water; refraction must be considered.

Actually, the problem is even more difficult because of the dispersive property of waves, combined with their non-uniform characteristics. The various components refract in an appropriate manner; hence the wave motion on the water surface is transforming in a direction perpendicular to the direction of propagation as well as in the direction of propagation. Fortunately, in the more shallow water near beaches this dispersive problem becomes less acute.

Considerable theoretical studies have been made in regard to the problems due to the dispersive properties of ocean waves. These studies have been compared with results obtained in the laboratory. In addition, arrangements were made with the Santa Cruz Portland Cement Company for the use of their pier (located at Davenport, California) - Figure 12, and four step-resistant gages were ordered from the Beach Erosion Board for installation along the pier. These have just been delivered, and a detailed field program will commence shortly.

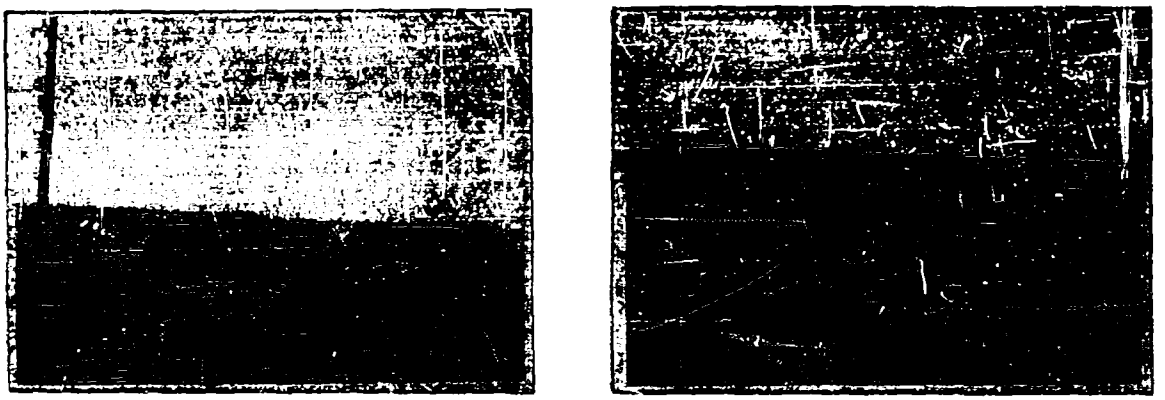

2230 GCT
17 Jan 1945

PHOTOS OF SEA SURFACE

1915 GCT
20 Jan 1945

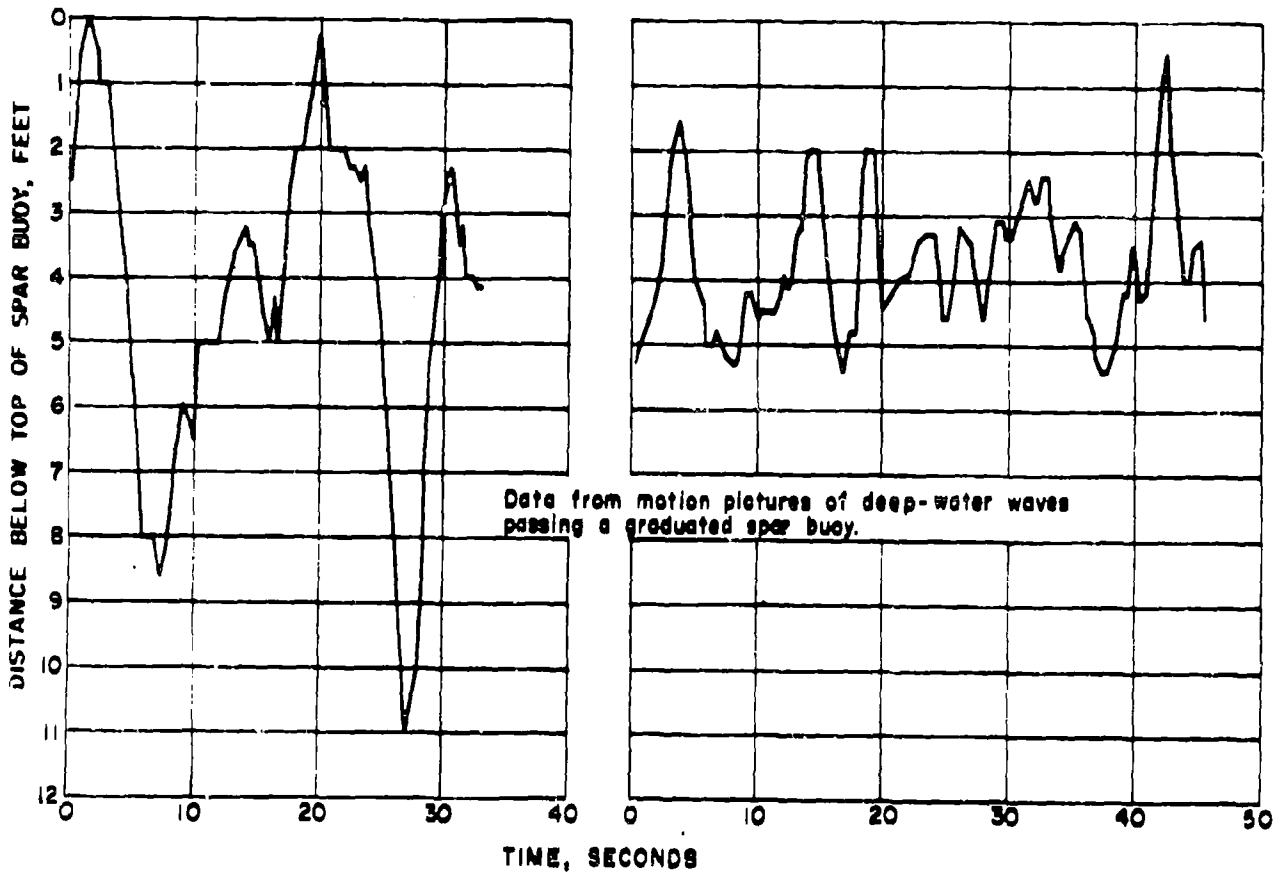

Data from motion pictures of deep-water waves passing a graduated spar buoy.

Swell:
H_{ave} = 4.5 ft., T = ——
Wind Waves:
H_{ave} = 3 ft., T = 6 sec.

2230 GCT, 17 Jan 1945

Swell:
H_{ave} = 6.6 ft., T = 12.8 sec.
Wind Waves:
H_{ave} = —— T = 5.5 sec.

1915 GCT, 20 Jan 1945

FIGURE 1

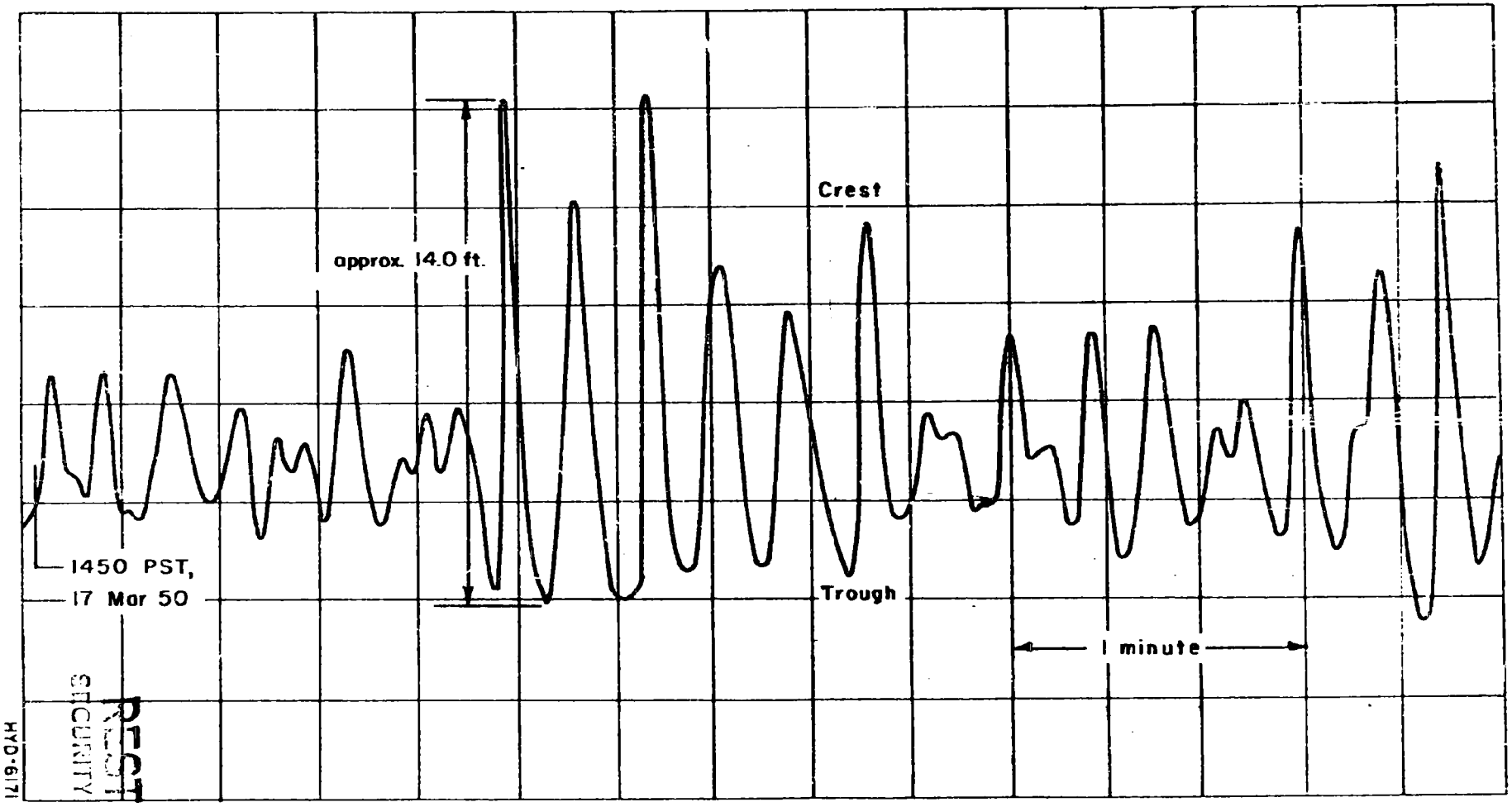

HYD-617

RESTRICTED
SECURITY INFORMATION

Plate 2

SURF VARIABILITY

COPY OF WAVE RECORD FROM MARK V PRESSURE HEAD
IN 20 FEET OF WATER, SOLDIERS CLUB BEACH, FORT ORD, CALIFORNIA

a Long-crested waves

b. Medium-crested waves

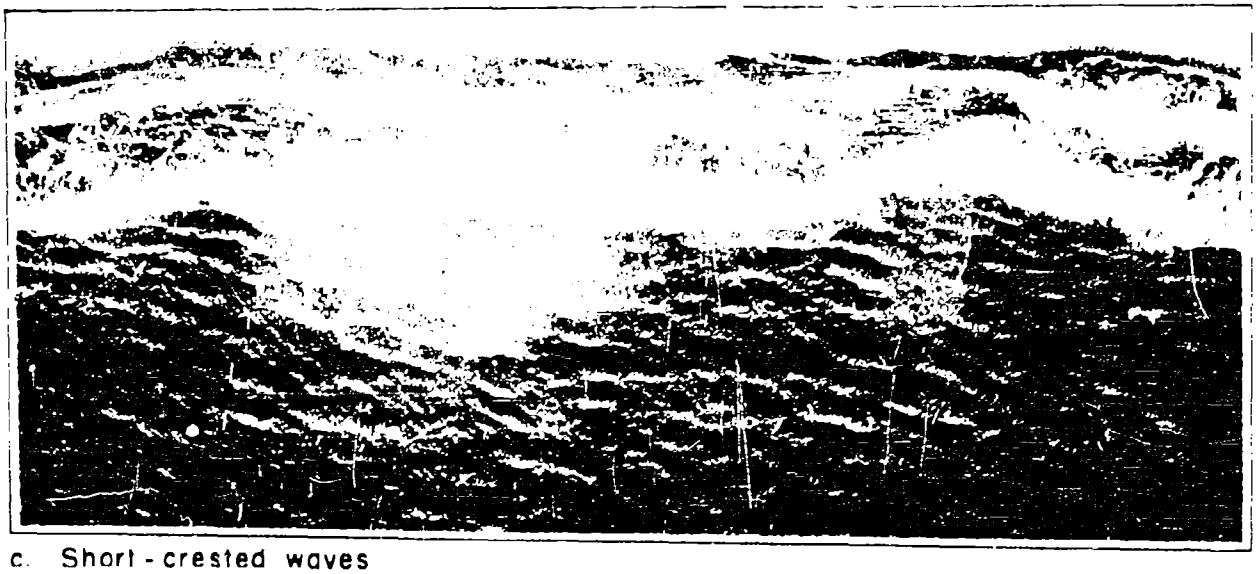

c. Short-crested waves

FIGURE 3

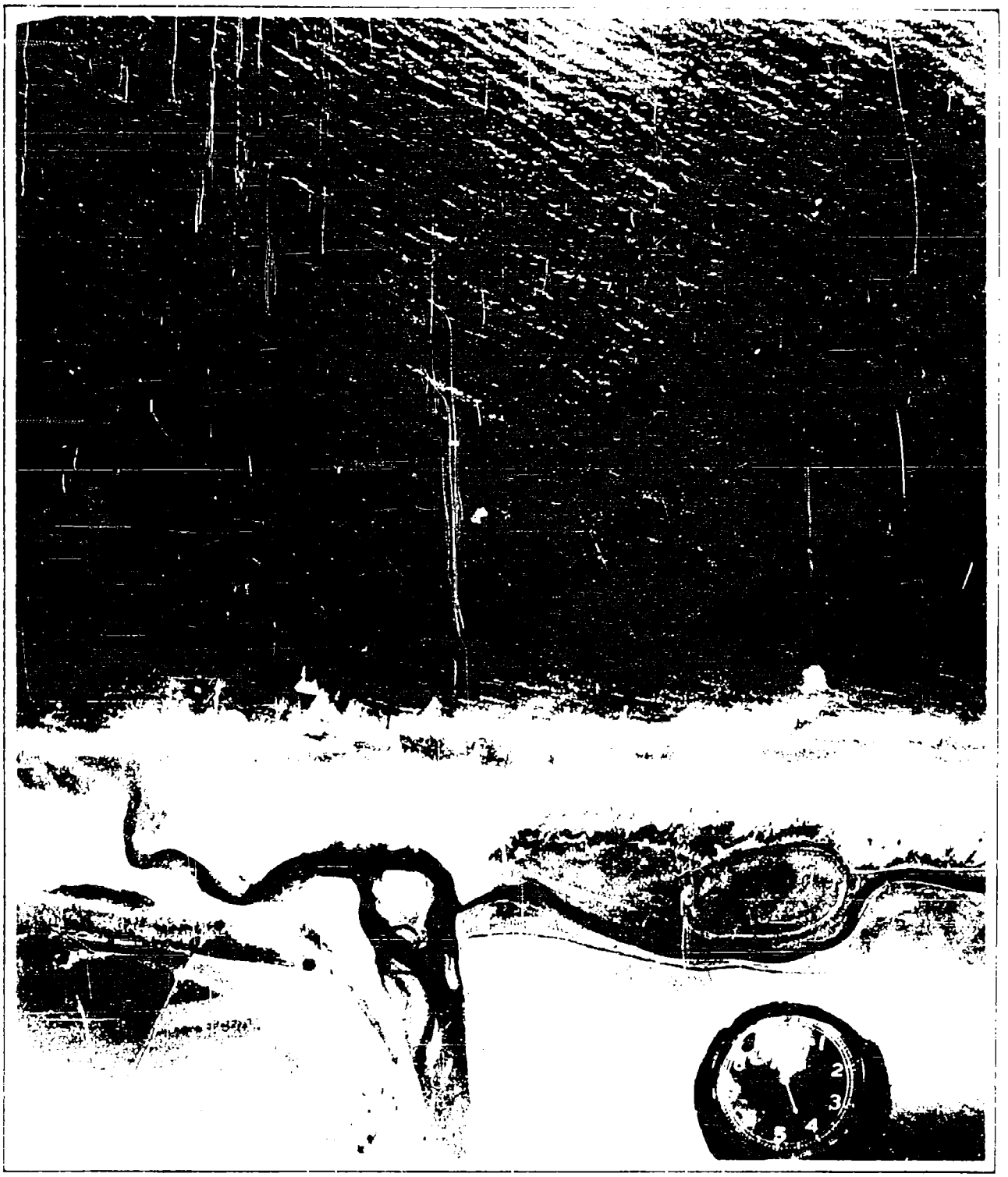

REFRACTION OF SHORT-CRESTED WAVES
AT ELKHORN SLOUGH, CALIFORNIA

FIGURE 4

B. LABORATORY STUDIES

Wave Channel: The laboratory experiments were performed in a wave channel, 1 foot wide, 60 feet long and 3 feet deep located in the Fluid Mechanics Laboratory of the University of California, Berkeley. The front side of the channel consisted of plate-glass, framed in 3 ft. x 3 ft. steel frames, through which motion pictures of the wave transformation were taken. The wave generator, of the flapper type, was located at one end of the channel. Both the amplitude and period of the flapper movement were adjustable. The period of the flapper movement could be varied between approximately 0.4 seconds and 2 seconds. At the opposite end of the channel from the wave generator an aluminum beach was installed for the purpose of eliminating reflected waves.

Transformation of Finite Wave Groups in a Uniform Depth of Water: Wave groups were generated by operating the flapper manually for the shorter wave groups and mechanically for the longer groups. Manual operation gave both better control of the number of waves, and a more uniform wave period. It was found when operating the generator mechanically that it took approximately 8 waves before the generator was accelerated to a constant period, and that at the end of the run the flapper did not stop as soon as the motor was turned off. Hence, mechanical operation of the flapper resulted in wave groups with long waves at the start, then a gradual decrease in wave length (becoming constant in length), and then after the motor was stopped, a gradual increase in wave length again, until the flapper completely stopped.

The initial groups studied contained from 1 to 25 waves. The surface-time histories were recorded at 4 locations along the channel with the first element 1 foot from the generator, the second 11 feet, the third 21 feet and the fourth 31 feet. The water depth was uniform and equal to 2.0 feet (at elements 1, 2 and 3) from the flapper to the toe of the beach. It was 1.6 feet at element 4, which was located landward of the toe of the beach. The beach slope was 1:15.

The surface-time histories were recorded by use of double-wire resistance elements* connected to Brush recorders. The data on these recorders were correlated by connecting them to a switch operated by the wave generator, at station 0+00. The flapper passing the switch the first time closed it, causing a mark to be placed on the records, thus affording a "zero time". Figure 5 illustrates one of the runs (No. 94) with the flapper of the wave generator moved twice back and forth, with a result of two waves in the initial group one foot from the generator. In this figure the transformation of the wave group as it advances down the channel can readily be seen.

Knowing the surface elevation-time history at one location it is possible to predict the water surface at the other locations. This has been done and the results compared with the theory, with good agreement. The results are presented in subsequent sections of this report.

Wave Transformation of Non-uniform Waves in Uniformly Shoaling Water: The experiments just described were performed to check the theory for prediction in water of uniform depth. But the important problem in most practical cases is to predict wave transformation in shoaling water. Hence, a beach with a uniform slope of 1:40

*Morison, J.R. "Measurements of Heights by Resistance Elements". The Bulletin, Beach Erosion Board, Corps of Engineers, vol. 3, no. 3, pp. 16-22; 1949.

was installed. Because of the limited length of channel a water depth of only 1.17 feet was used. This left a section of uniform depth 10.42 feet long between the toe of the beach and the wave generator, which allowed the waves to stabilize before reaching the toe of the beach. The water line on the beach was 57.80 feet from the wave generator.

Wave groups were generated by moving the flapper manually in order to mix periods and amplitudes. In addition to the finite wave groups, measurements were made for steady-state uniform waves by generating the waves mechanically and taking the measurements only after a steady state was reached. The water surface-time history was recorded at two locations. The first element was located just landward from the toe of the beach (10.42 feet from the flapper) with the water depth $d_1 = 1.17$ feet. The second element was located 41.62 feet from the flapper, with $d = 1/3\ d_1 = 0.39$ foot.

As far as the uniform trains of waves were concerned, it was easy to identify the same wave on both records and to determine the number of waves between the elements. However, difficulties arose in the case of trains of non-uniform waves. Some of the waves would disappear and new waves appear; so, it was not always possible to identify the same wave on different records. Unfortunately, records of this sort do not show the continuous change of a train of irregular waves even when the points of measurement are numerous and close together. As this was very important to the understanding of the problem, it was decided to obtain a continuous record of irregular waves with movies. Four 35 mm. Bell & Howell "Eymo" cameras (25 mm. focal length f. 2.8 lens) were used, each one having a coverage of 9 feet. The cameras were operated simultaneously, overlapping each other's field of view.

In order to obtain a time-scale for the measurements, and to correlate the data of the different cameras, three clocks were used. Two of the clocks were graduated in 0.01 second increments (one sweep of the arm equal to 1 second) and one in 0.01 minute (1 sweep equal to 1 minute). The arrangement of the set-up is shown in Figure 8. The clock graduated in 0.01 minute increments (clock 2 in the sketch) was used only to correlate the readings of clocks 1 and 3.

The measurements obtained from the motion pictures were checked by placing a double wire resistance element in the view of Camera III at a known location, and measuring the surface-time history by means of a Brush recorder at the same time that the movies were being taken. To correlate the data of the Brush recorder and the movies, the connections to the clocks were made through the Brush recorder so that the moment the clocks were started a mark was placed on the record. Agreement between the data obtained from the movies and that from the Brush record was found to be very good.

Experimentation with the photography showed that clear water gave a surface line in the photographs which was difficult to read. There appeared to be several methods of overcoming this and thereby obtain a clear image of the surface profile in the pictures. It was decided to cover the glass windows in the channel with tracing paper, stretched tightly against the surface of the glass. A grid, with 0.01 foot divisions, was drawn on the paper to obtain a scale for the evaluation of the data, and the distances from the wave-generator indicated. When a strong light was directed to the water surface a very clearly distinguished shadow line was obtained on the tracing paper; hence, the shadow of the water-surface profile was actually photographed. The results were satisfactory. Special care was taken

to keep the tracing paper as tight as possible to the glass; otherwise the shadow image would not be clear and would result in erroneous readings.*

The duration of the run was approximately 90 seconds, as this was considered to be adequate from a statistical standpoint.

The movies were analyzed frame by frame, each wave in the photographs being assigned a number, and the time and location of these waves being measured as the waves advanced down the channel. The procedure was very tedious and the evaluation of the data has not yet been completed. The data obtained were plotted as time versus distance traveled. Hence, the distance between waves in the vertical direction gives the wave periods at any desired time and location, the distance between waves in the horizontal direction gives the wave lengths, and the slopes of the curves give the wave velocities. A sample of the data, from Camera I, is shown in Figure 7. These are the waves in the deepest water; hence the time-distance curves are almost straight lines. It is expected that the curvatures would increase as they come into shallower water and the velocities of the wave travel decrease.

The evaluation of the data is not yet advanced enough to discuss fully the results, but looking at Figure 7 it is interesting to note that when a wave disappears, there appears a new wave a short distance to the rear of the previous wave. This is demonstrated by Wave 88, which disappears at Station 33 and is replaced at Station 34 by Wave 87-A. The same characteristics can be found for Waves 87 and 83. Wave 87 breaks and disappears and is replaced a short distance later by another wave. Waves 88 and 87-A, and 87 and 86 demonstrate the mixing of two waves. In the case of Waves 88 and 87-A, the two crests merge, becoming a long, flat-crested wave, with no distinguishing maximum (see Figure 7, Stations 33-34). The single crest then separates into two crests again, one of which soon disappears. In the case of Waves 87 and 86 a different phenomenon occurs: Wave 87 breaks, and water rolls forward merging with Wave 86 and forming a long, flat-crested wave. As in the case of Waves 88 and 87-A this separates into two waves, one of which soon disappears.

In Figures 8-10 are shown a series of sketches of the wave profiles as they moved down the channel. Each sketch shows nearly the entire shoaling section. The time interval between each sketch varies.

Wind Waves in Uniformly Shoaling Water: Several laboratory experiments were performed in order to determine the characteristics of wind generated waves. The channel was covered to form a wind tunnel with the water as the bottom boundary of the wind. A sloping beach was placed at one end of the channel. The wind was forced through the tunnel over the water and toward the beach. The resulting waves were measured simultaneously at three stations along the sloping beach. Figure 11 shows a sketch of the experimental set-up.

The analysis of these data will show the effect of shoaling on wind waves together with their transformation in the generating area due to their dispersive properties. The results will be presented in a subsequent report.

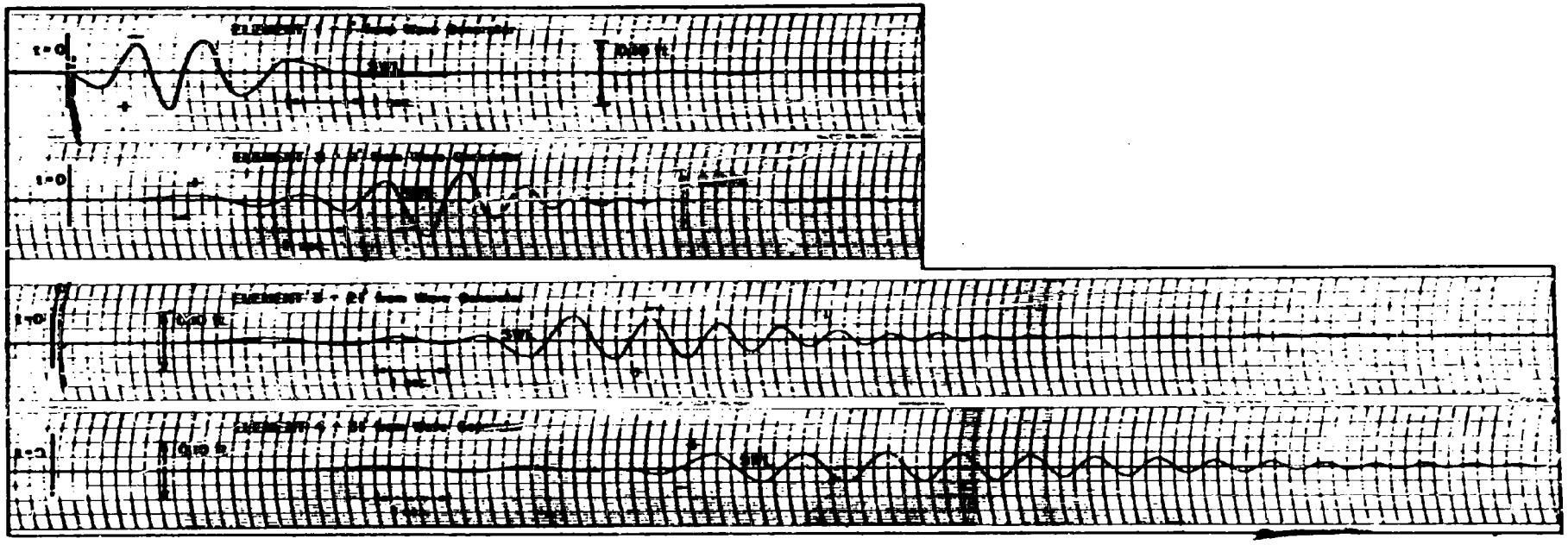

Waves generated by moving the flapper back and forth twice

WAVE TRANSFORMATION - RUN 94

FIGURE 5

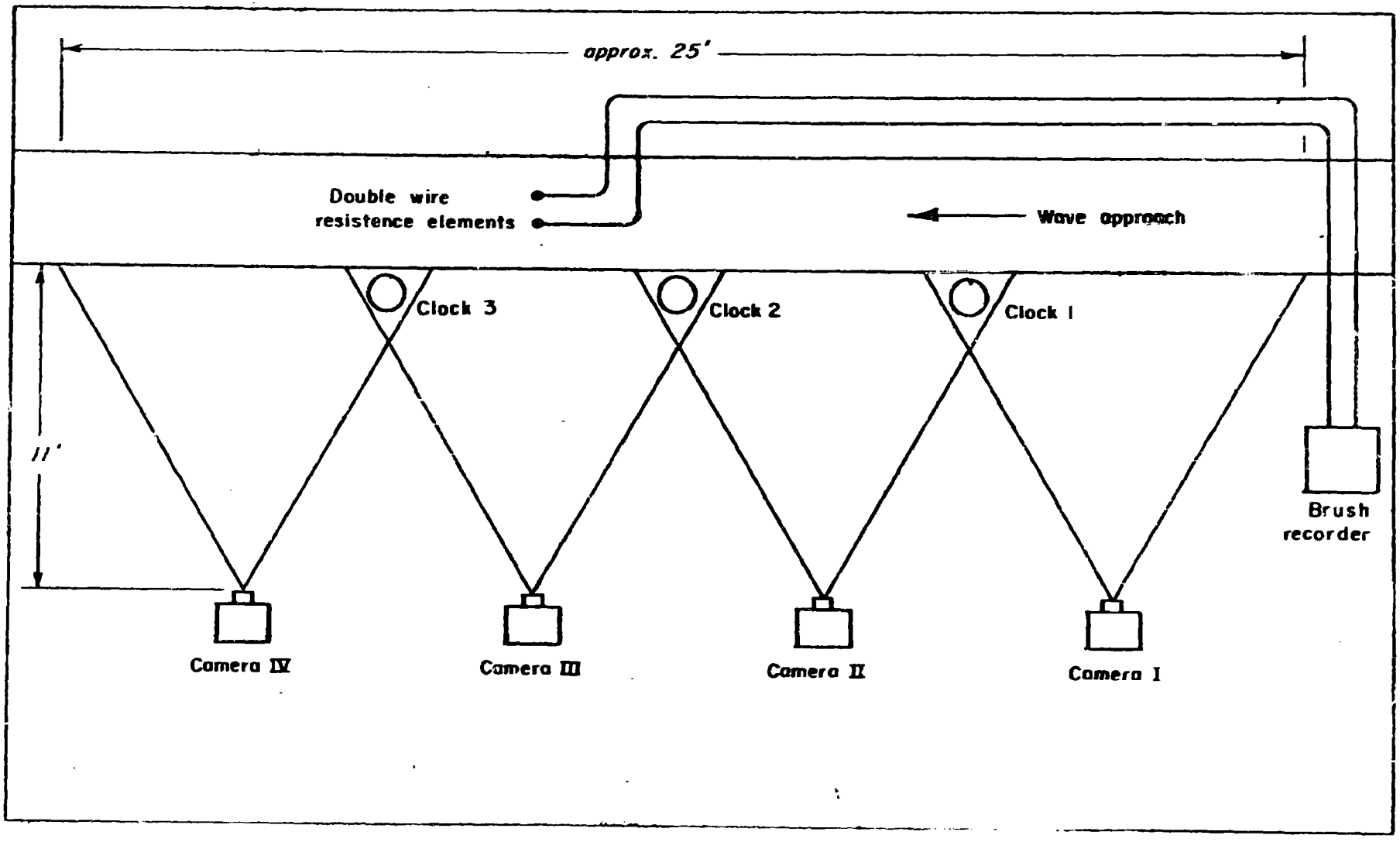

SKETCH OF THE SET-UP

Figure 8

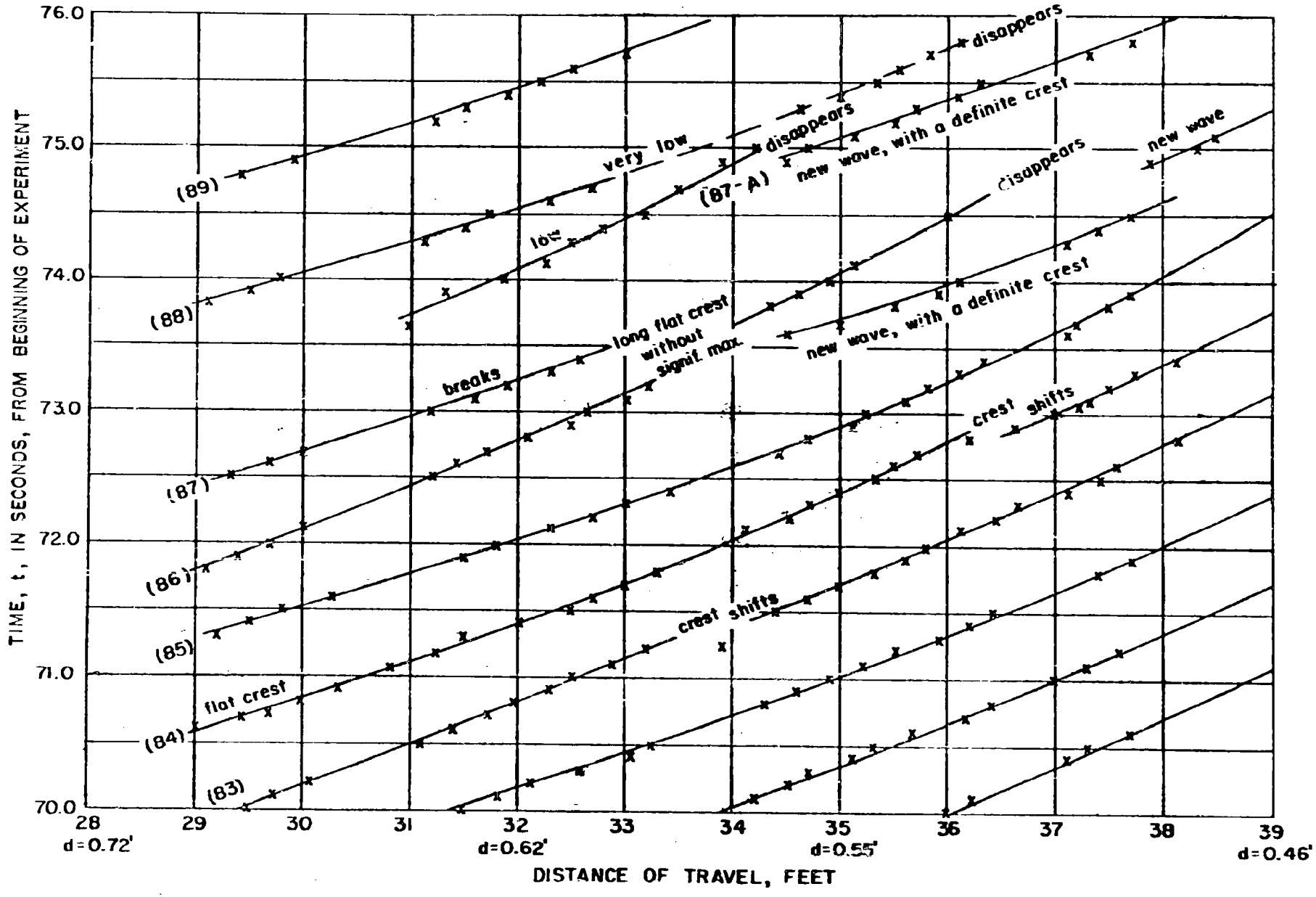

FIGURE 7 WAVE TRANSFORMATION - IRREGULAR TRAIN OF WAVES

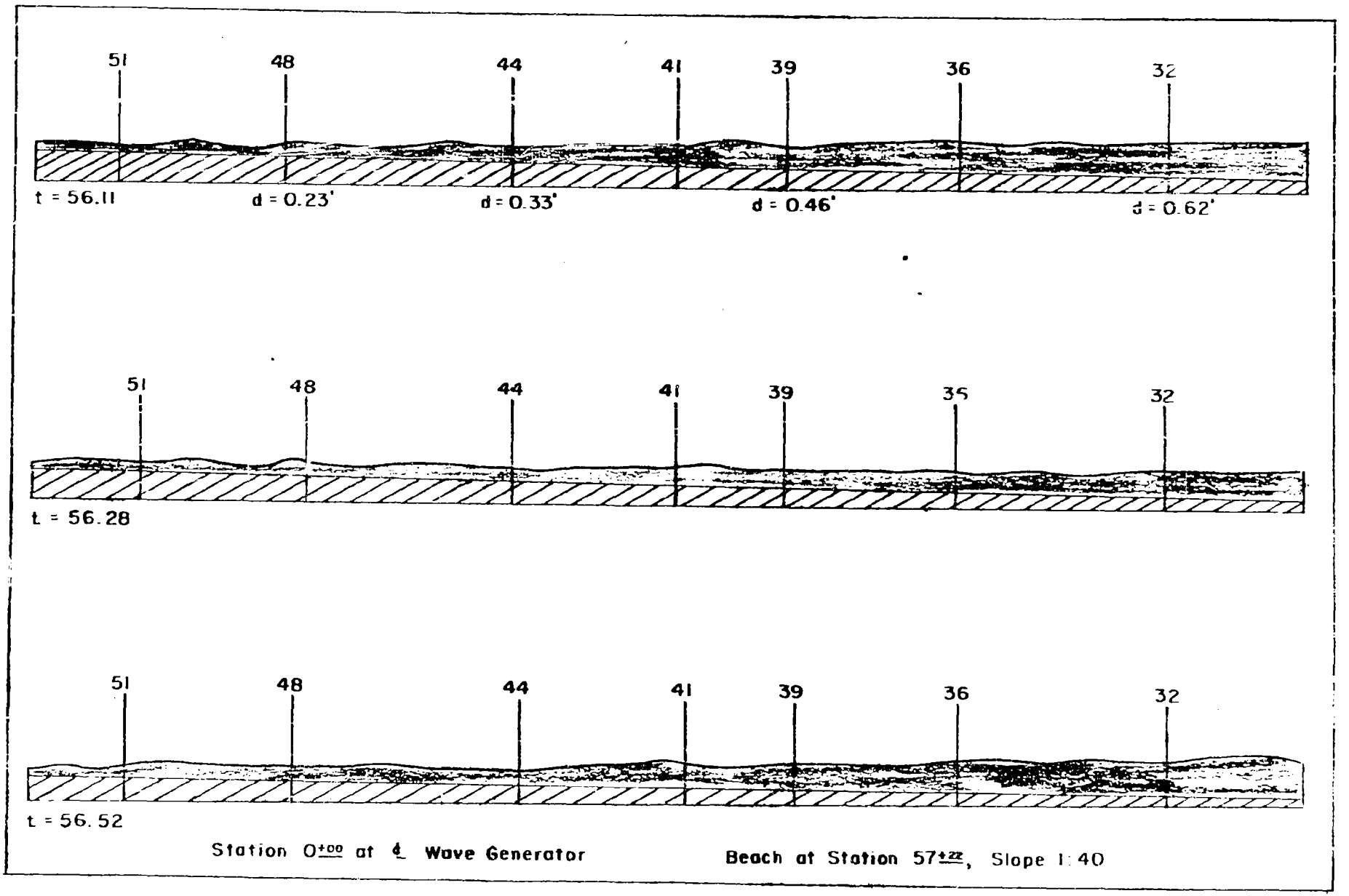

WAVE TRANSFORMATION – IRREGULAR WAVES

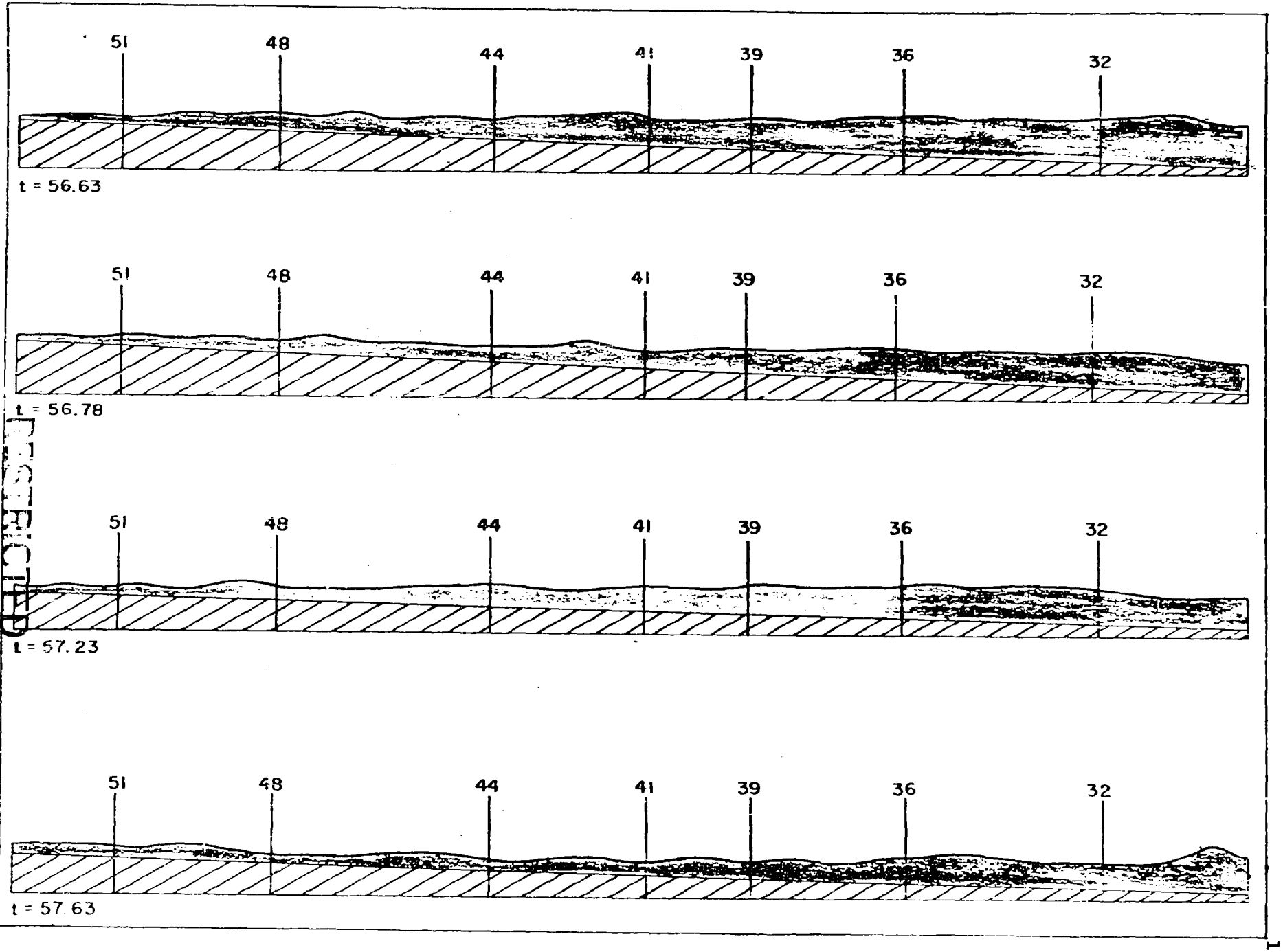
51
48
44
41
39
36
32
t = 56.63
51
48
44
41
39
36
32
t = 56.78
51
48
44
41
39
36
32
t = 57.23
51
48
44
41
39
36
32
t = 57.63

Figure 10

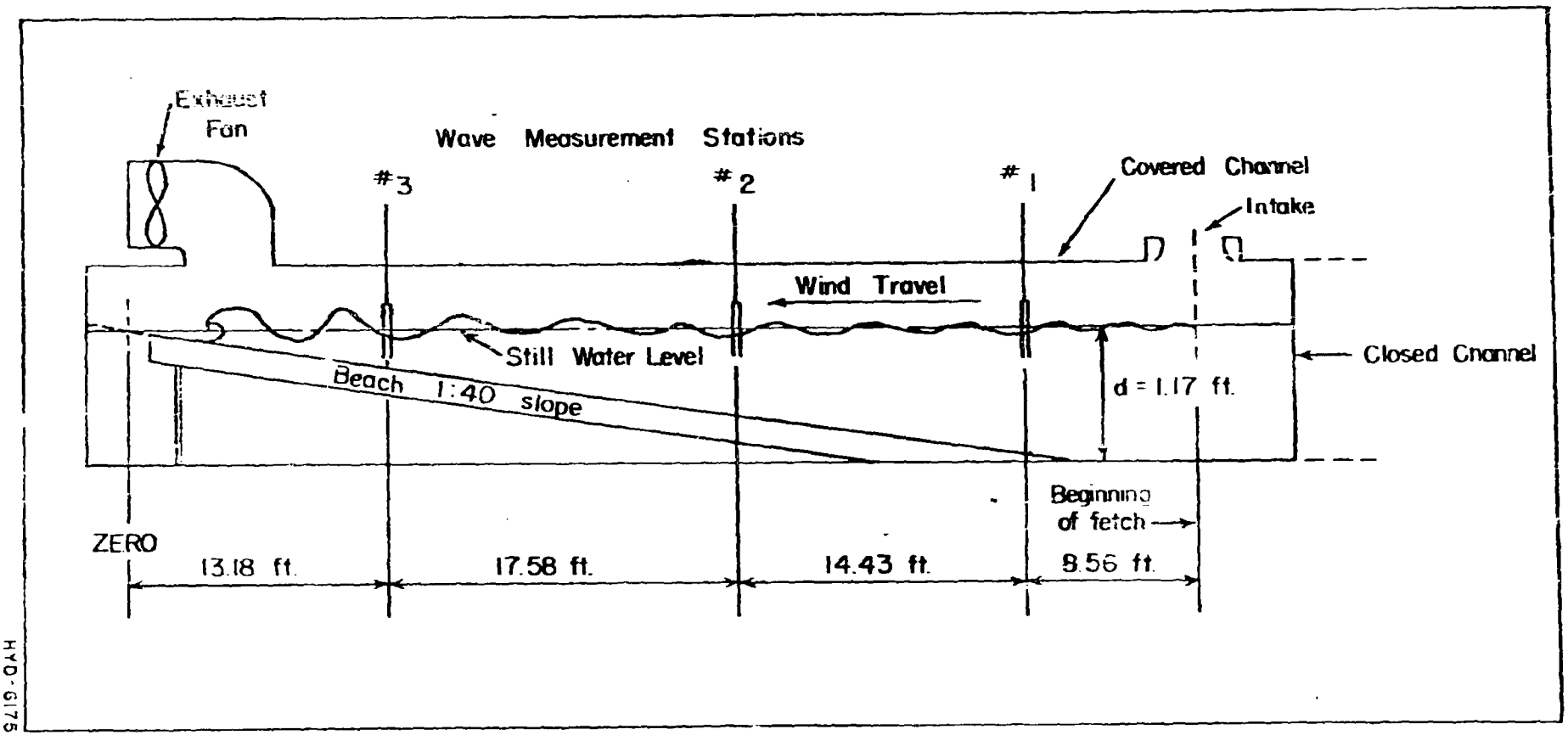

FIGURE 11 – SCHEMATIC DIAGRAM OF EXPERIMENT ON WIND WAVES IN UNIFORMLY SHOALING WATER

C. FIELD STUDIES

Field Work at Davenport, California: Through the cooperation of the Santa Cruz Portland Cement Company, the University of California has been given permission to use an abandoned cement loading pier at Davenport, California for studying wave transformation (Figure 12). The pier is unusually long (2200 feet) and is constructed in an exposed location on the coast, giving an excellent chance for the study of long period large waves from the North Pacific area.

Moving pictures were taken of waves moving along the pier in an initial effort to define the complexity of the transformation problem. It was found that waves could be tracked visually from the end of the pier to shore and that the travel times of these waves could be predicted satisfactorily from theoretical considerations. Work is now going on in preparation for an extensive wave measurement program correlating waves along the pier and waves a mile westward of the pier end. It is planned to install four Beach Erosion Board step-resistance gages along the pier to record the transformation of waves in shallow water and to install a network of wave pressure recorders one mile off shore in a depth of 80 feet to measure the deep-water waves coming into shore.

It has been necessary to install new walkways along the pier and also to put in electric service and communication lines since some of the pier superstructure has rotted or washed away and much of the original equipment has been removed. A wave pressure recorder was put into operation at the pier end to give some idea of the wave size and period to be expected during the proposed tests.

Field work at Ellwood: In connection with the problem of wave transformation, two preliminary tests were made at Ellwood, California on a pier owned by Signal Oil and Gas Company. The tests consisted of spacing two wave pressure recorders a distance of 28.5 and 205 feet apart, near the surface and on a line with the direction of approach of the waves. The water depth at the seaward recorder 2200 feet from shore was 35 feet. Analyses of the data obtained from these tests are described in Sections F and G.

D. LINEAR PREDICTION IN WATER OF CONSTANT DEPTH

In a previous report* the predicted surface elevation at a distance x in the direction of wave propagation was shown to be of the form

$$E(t) = \int_{-\infty}^{\infty} E(\tau - t)\, K(\tau)\, d\tau$$

where $K'(t) = \frac{1}{\pi} \int_0^{\infty} \cos(Kx - \sigma t)\, d\sigma$ and $\sigma^2 = g K \tanh K d$. For deep water we find explicitly

$$K'(t) = \frac{1}{2\pi}\sqrt{\frac{\pi g}{x}} \cos\left(\frac{\pi}{4} - \frac{gt^2}{4x}\right).$$

which is plotted vs. t for x = 10 in Figure 13. In general this surface kernel can be written in the form

$$K'(t) = \frac{1}{\pi}\sqrt{\frac{g}{d}} \int_0^{y_m} \cos\left(u\frac{x}{d} - vy\right) dy$$

where $y^2 = u \tanh u$, $u = kd$, $y = \sqrt{\frac{d}{g}}\,\sigma$, $v = \sqrt{\frac{g}{d}}\,t$.

Calculations have been performed for $\frac{x}{d} = 5$ and $y_m = 2, \infty$. This last set of values implies the neglect of component periods of less than $\frac{2\pi}{y_m}\sqrt{\frac{d}{g}}$ or the consideration of d/L values less than 0.64, ∞ respectively. The integral has been calculated using Filon's formula. The results are plotted in Figure 13.

Successive predictions were made for d = 2 feet and stations 10 feet apart the first being one foot from the wave paddle. The results are indicated in Figure 14 for an initial finite sine wave the first record being taken one foot from the wave flapper. The results at Station 3 were predicted from the measured surface-time history at Station 2 and the prediction for Station 4 was made from the measured surface-time history at Station 3. In Figure 15 a single prediction is made for a larger number of initial oscillations. Trial predictions were made for data secured at Ellwood but since the experimental conditions did not conform to those used in the calculations no comparison will be offered.

*Institute of Engineering Research, Univ. of Calif., Series 3, Issue 337, June 1962

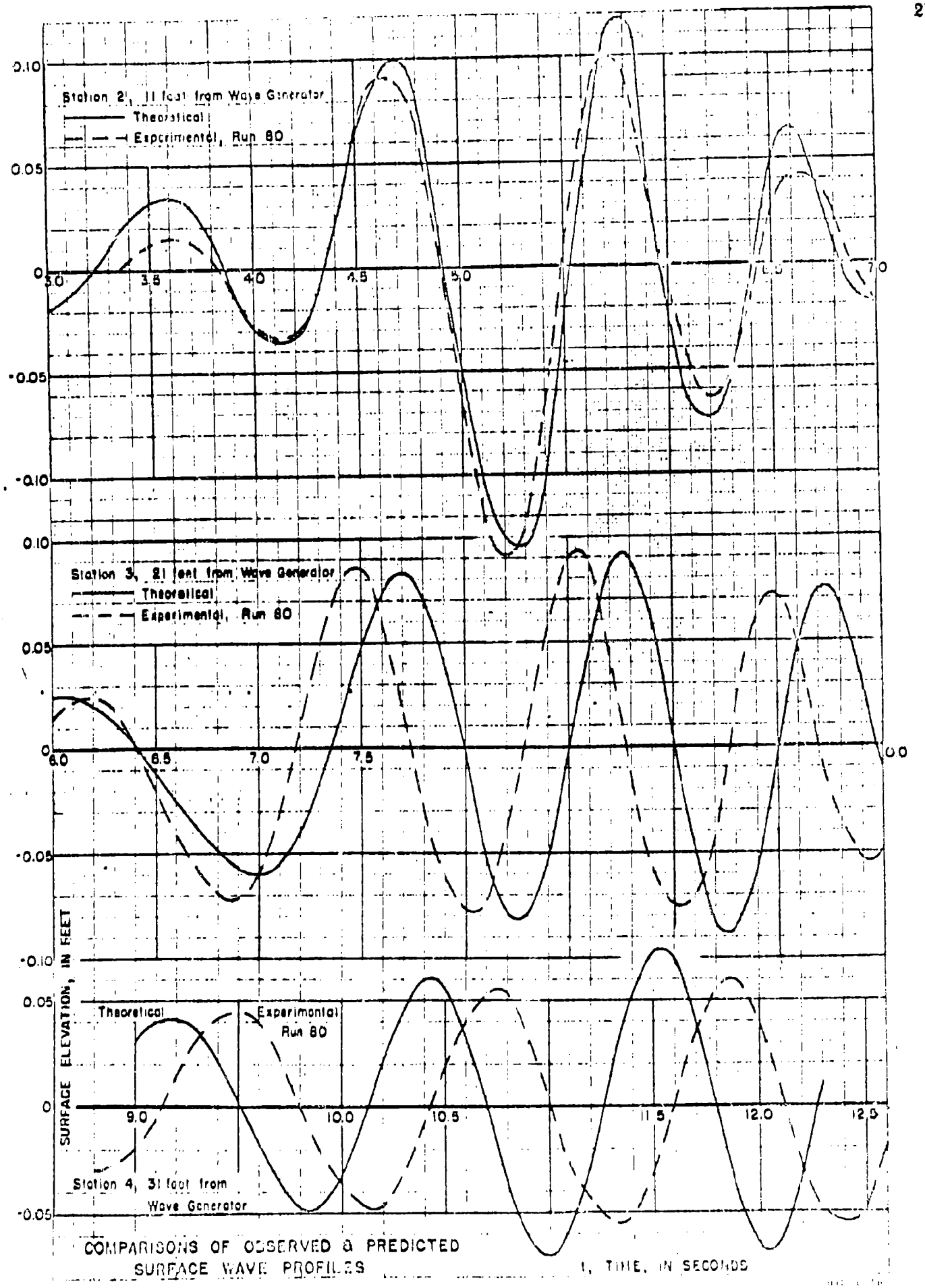

COMPARISONS OF OBSERVED & PREDICTED SURFACE WAVE PROFILES

FIGURE 14

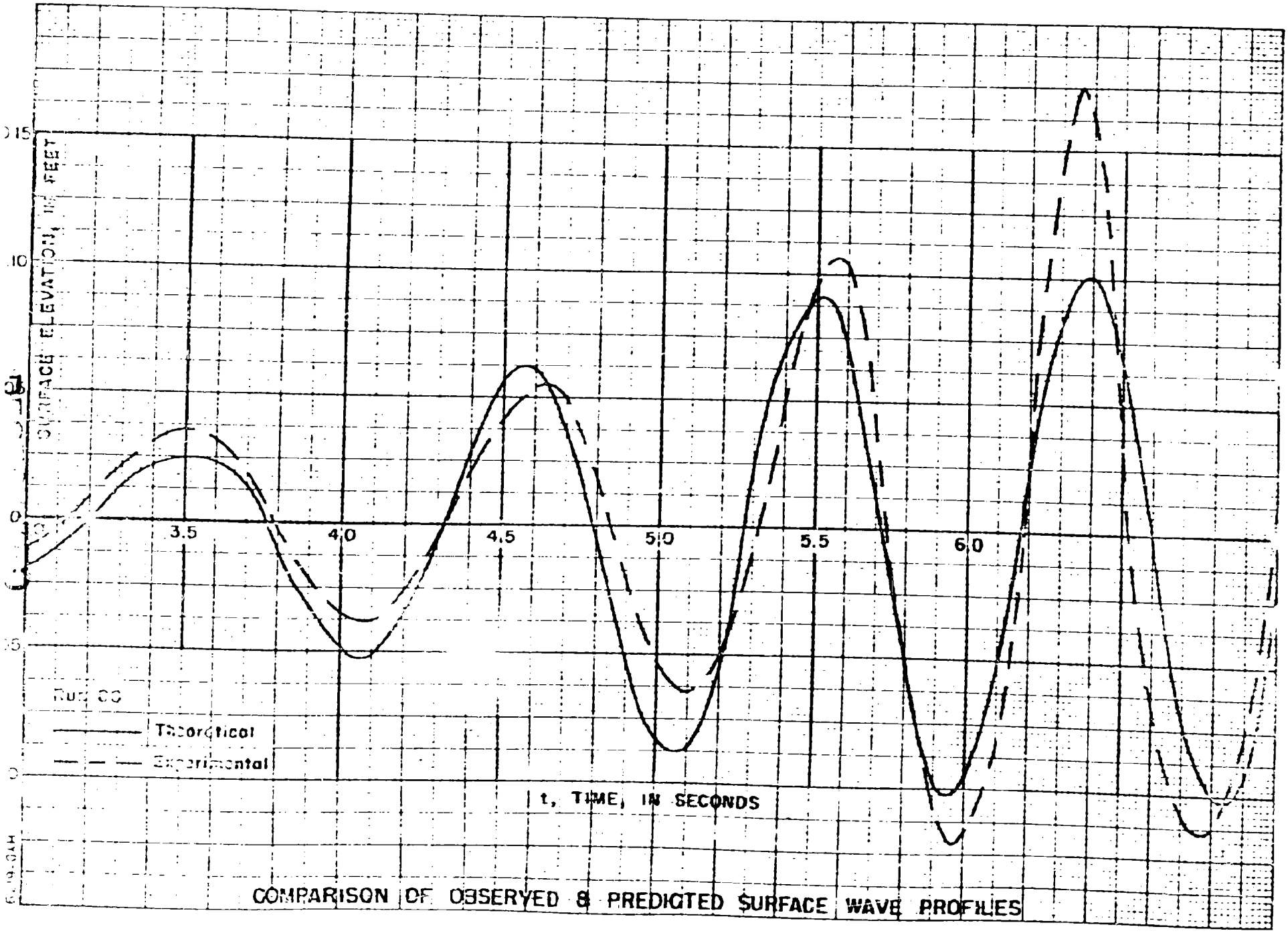

COMPARISON OF OBSERVED & PREDICTED SURFACE WAVE PROFILES

E. LINEAR PREDICTION OF WAVE TRANSFORMATION ON BEACHES OF CONSTANT SLOPE

In order to generalize the prediction of wave transformation from water of constant depth to shoaling water one must in general take account of changes in phase, amplitude and refraction angle. For simplicity we shall consider beaches of uniformly constant slope with waves moving directly onshore and having crests parallel to the bottom contours. We assume that a periodic wave has an amplitude which is determined by Rayleigh's hypothesis of the conservation of transmitted power and the phase is determined by suitably integrating the instantaneous wave number appropriate to the depth.*

For transformation from depth d_2 with wave amplitude a_2 to depth d_1 with amplitude a_1 as shown below

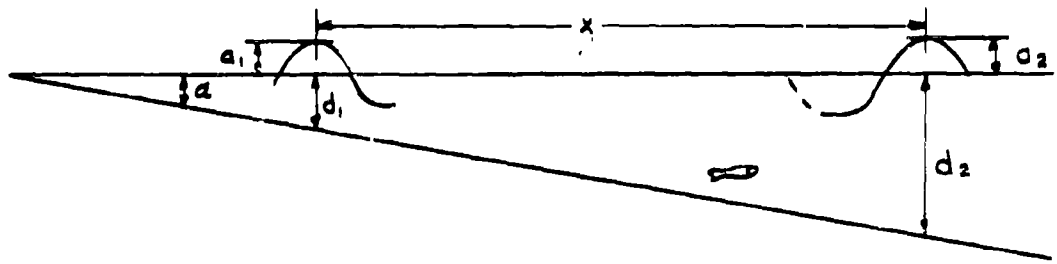

we find

$$\frac{a_1}{a_2} = \frac{a_1}{a_o} \quad \frac{1}{a_2/a_o} = \sqrt{\frac{n_2\, c_2}{n_1\, c_1}}$$

where the subscript o refers to deep water and

$$n = \frac{1}{2}\left(1 + \frac{2\,k\,d}{\sinh 2kd}\right)$$

$$\frac{c}{c_o} = \frac{L}{L_o} = \tanh k\,d$$

$k = \frac{2\pi}{L}$, L being the wavelength.

For a periodic wave of frequency the surface profile is of the form

$$\eta(t) = a\,(t)\cos\left(\lambda(d) - \sigma t\right)$$

where

$$\lambda(d) = \int_0^x k\,dx$$

*Manual of Amphibious Oceanography, Wave Theory, Sec. II. p. 63

x being measured plus toward shore with x = o at depth d_2.

For a continuous sequence of underlying frequencies we generalize this simple formula by integration over σ in order to gain Fourier integral representations. Thus

$$\eta_2(t) = \int_{-\infty}^{\infty} a_2(\sigma)\, e^{-i\sigma t}\, d\sigma \qquad (1)$$

where $\sigma^2 = g k \tanh k d$. Inverting (1) by Fourier's integral theorem the spectral amplitude is

$$a_2(\sigma) = \frac{1}{2\pi} \int_{-\infty}^{\infty} \eta_2(u)\, e^{i\sigma u}\, du.$$

At a distance x

$$\eta_1(t) = \int_{-\infty}^{\infty} a_1(\sigma)\, e^{i(\lambda(d_1) - \sigma t)}\, d\sigma$$

$$= \int_{-\infty}^{\infty} \frac{a_1}{a_2}\, a_2\, e^{i(\lambda(d_1) - \sigma t)}\, d\sigma$$

$$= \frac{1}{2\pi} \int_{-\infty}^{\infty}\int_{-\infty}^{\infty} \sqrt{\frac{n_2 c_2}{n_1 c_1}}\, \eta_2(u)\, e^{i[\sigma(u-t) + \lambda(d_1)]}\, d\sigma\, du$$

$$= \int_{-\infty}^{\infty} \eta_2(u)\, K(u - t)\, du$$

$$= \int_{-\infty}^{\infty} \eta_2(t - v)\, K(v)\, dv$$

where $K(v) = \frac{1}{2\pi} \int_{-\infty}^{\infty} \sqrt{\frac{n_2 c_2}{n_1 c_1}}\, \cos(\lambda(d_1) - \sigma v)\, d\sigma$

Applying the method of stationary phase to this integral results in the approximate formula

$$K(v) = \frac{\sqrt{\pi}\, \sqrt{\frac{n_2 c_2}{n_1 c_1}}}{\sqrt{\frac{1}{2}\frac{d^2\lambda}{d\sigma^2}}} \cos(\lambda(d) - \sigma v + \pi/4)$$

Calculations using this approximation were performed for $\alpha = 1/40$, $d_1 = 0.39$ ft. and $d_2 = 1.17$ ft. corresponding to experimental conditions described elsewhere in this report. Numerical calculations were carried out for the range of periods between 0.36 and 1.26 sec. which appeared to cover the range of experimental conditions. The results are given numerically in Table 1. The amplitude $f(v)$ and the phase $g(v)$ are plotted separately in Figure 16. Predictions employing this kernel are compared with experiment in Figures 17a and b. Discrepancies between theory and experiment are in part attributable to the approximations involved in employing the method of stationary phase.

TABLE I

KERNEL FOR WAVE TRANSFORMATION

v	K(v)	v	K(v)	v	K(v)	v	K(v)
9.4	-1.51	15.2	-1.48	31.0	-0.82	26.8	-0.54
9.6	0.93	15.4	-0.21	21.2	1.46	27.0	-0.03
9.8	2.01	15.6	1.53	21.4	-1.36	27.2	0.61
10.0	0.24	15.8	-0.59	21.6	0.38	21.4	-1.12
10.2	-1.82	16.0	-1.21	21.8	0.84	27.6	1.49
10.4	-1.27	16.2	1.23	22.0	-1.54	27.8	-1.70
10.6	1.04	16.4	0.56	22.2	1.24	28.0	1.73
10.8	1.79	16.6	-1.51	22.4	-0.14	28.2	-1.71
11.0	-0.26	16.8	0.24	22.6	-1.06	28.4	1.63
11.2	-1.85	17.0	1.38	22.8	1.57	28.6	-1.51
11.4	-0.48	17.2	-0.98	23.0	-1.36	29.0	1.32
11.6	1.62	17.4	-0.63	23.2	0.58	29.2	-1.10
11.8	1.12	17.6	1.51	23.4	0.45	29.4	0.83
12.0	-1.13	17.8	-0.63	23.6	-1.30	29.6	-0.57
12.2	-1.36	18.0	-0.98	23.8	1.62	29.8	0.54
12.4	0.98	18.2	1.44	24.0	-1.25	30.0	-0.50
12.6	1.41	18.4	-0.24	24.2	0.35	30.2	0.46
12.8	-0.84	18.6	-1.24	24.4	0.70	30.4	-0.43
13.0	-1.45	18.8	1.28	24.6	-1.33	30.6	0.39
13.2	-0.69	19.0	0.16	24.8	1.64	30.8	-0.35
13.4	1.48	19.2	-1.33	25.0	-1.53	31.0	0.32
13.6	-0.59	19.4	1.31	25.2	1.05	31.2	-0.30
13.8	-1.39	19.6	-0.12	25.4	-0.30	31.4	0.54
14.0	0.90	19.8	-1.18	25.6	-0.54	31.6	-0.76
14.2	1.18	20.0	.44	25.8	1.23	31.8	0.97
14.4	-1.16	20.2	0.41	26.0	-1.63	32.0	1.17
14.6	-0.91	20.4	-0.98	26.2	1.64	32.2	1.34
14.8	1.35	20.6	1.52	26.4	-1.43	32.4	-1.49
15.0	0.59	20.8	-0.70	26.6	1.04		

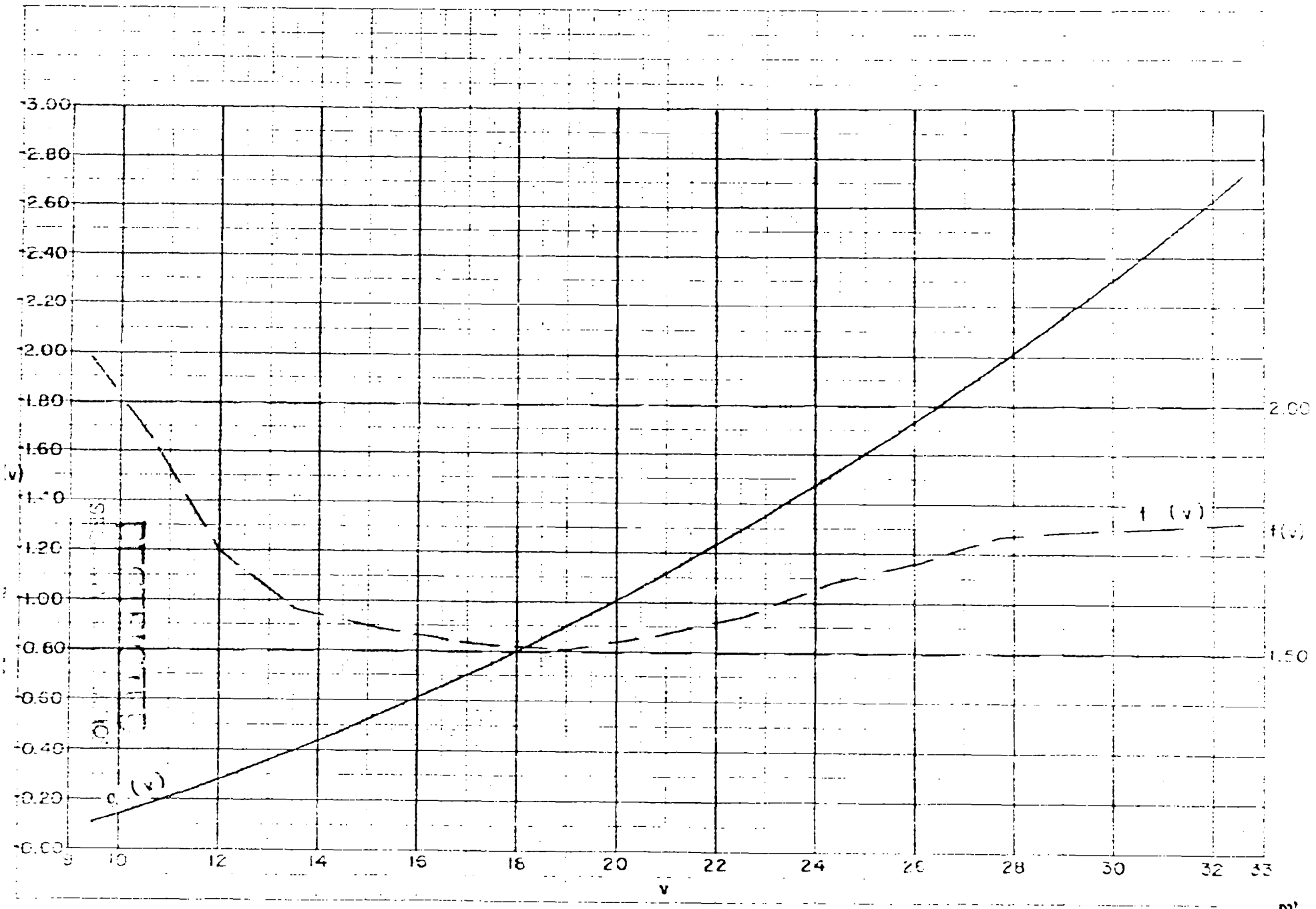

AMPLITUDE f(v) AND PHASE g(v) OF APPROXIMATE PREDICTION KERNEL K(v)

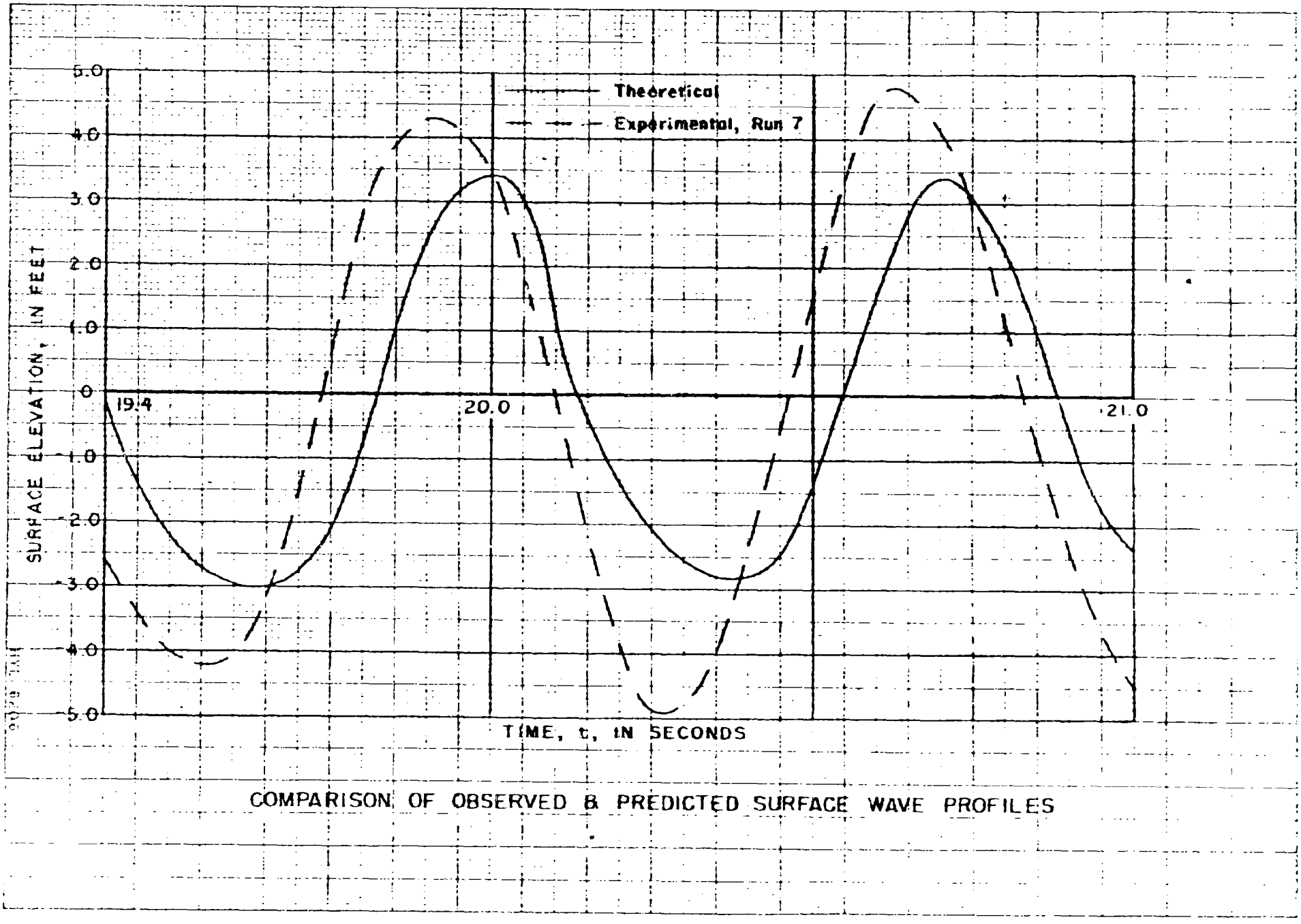

COMPARISON OF OBSERVED & PREDICTED SURFACE WAVE PROFILES

COMPARISON OF OBSERVED & PREDICTED SURFACE WAVE PROFILES
Predicted
Experimental, Run 6
SURFACE ELEVATION, IN FEET
TIME, IN SECONDS
19.0
15.0
14.0
11.0
23
25
26.0
21.0

F. FOURIER SERIES ANALYSIS

If the linear theory for wave propagation is adequate it should be possible to start with a record of the surface time history of wave motion at some point, and then after harmonically analyzing a section of this record into its various components, propagating the components separately in the direction of travel to some desired point and then recombine them. The point of reference on the longest component would arrive first at the point of interest while the reference point of the shortest component would arrive last. The recombined surface time history would begin to be valid only when the shortest components had started to arrive at the point of interest; hence the interval for which the surface time history can be predicted at this second point is always less than the length of record at the first point. If the section of record at the first point is relatively short and the distance between the two points is relatively long then no prediction from the first to the second is possible. This indicates that the greater the distance to the point of prediction the greater would be the section of measured record that must be harmonically analyzed. It follows that the longer the section of record harmonically analyzed the greater the number of harmonics necessary.

The basic limitations for the harmonic analysis method, as presented herein, are that the depth of water stays constant (the effect of shoaling is not included) and that the waves behave according to the linear wave theory. The mathematics involved in this method start with the representation of the measured surface by a Fourier Series which is given by the expressions

$$\eta_1(t) = a_0 + a_1 \cos \frac{2\pi t}{T_1} + a_2 \cos \frac{2\pi t}{T_2} + \ldots + a_n \cos \frac{2\pi t}{T_n}$$

$$+ b_1 \sin \frac{2\pi t}{T_1} - \ldots b_n \sin \frac{2\pi t}{T_n} \quad \ldots \qquad (1)$$

where

$\eta_1(t)$ = measured or known surface time history at point 1

$\eta_2(t)$ = computed surface time history at point 2 or any point other than point 1

$a_0, a_1, \ldots a_n, b_1, \ldots b_n$ - Fourier coefficient

t - time - seconds

n - number of sine or cosine components which is one-half the number of ordinates measured in the type of harmonic anaysis used*

τ = length of record harmonically analyzed in seconds

$T_1 = \tau$; $T_2 = \frac{\tau}{2}$ ...., $T_n = \frac{\tau}{n}$ = wave period of the component in seconds

ℓ = distance between point 1 and point 2 or any other point measured in direction of wave travel. Points must be in line in this direction.

---

*Den Hartog, J.P. "Mechanical Vibrations", McGraw-Hill Book Co., Inc. New York and London, 1940

Having obtained each component, they are now propagated to point 2 and recombine to give the following expression

$$\eta_2(t) = a_o + a_1 \text{ Cos } \frac{2\pi(t'+t_1-t_1)}{T_1} + a_2 \text{ Cos } \frac{2\pi(t'+t_1-t_2)}{T_2}$$

$$+ \cdots + a_n \text{ Cos } \frac{2\pi(t'+t_1-t_n)}{T_n} + b_1 \text{ Sin } \frac{2\pi(t'+t_1-t_1)}{T_1}$$

$$+ \cdots + b_n \text{ Sin } \frac{2\pi(t'+t_1-t_n)}{T_n} \quad \cdots \qquad (2)$$

which reduces to

$$\eta_2(t) = a_o + a_1 \text{ Cos } \frac{2\pi t'}{T_1} + \left[a_2 \text{ Cos } \frac{2\pi(t_1-t_2)}{T_2} + b_2 \text{ Sin } \frac{2\pi(t_1-t_2)}{T_2}\right] \text{Cos } \frac{2\pi t'}{T_2} +$$

$$\cdots + \left[a_n \text{ Cos } \frac{2\pi(t_1-t_n)}{T_n} + b_n \text{ Sin } \frac{2\pi(t_1-t_n)}{T_n}\right] \text{Cos } \frac{2\pi t'}{T_n} + b_1 \text{ Sin } \frac{2\pi t'}{T_1} +$$

$$+ \left[b_2 \text{ Cos } \frac{2\pi(t_1-t_2)}{T_2} - a_2 \text{ Sin } \frac{2\pi(t_1-t_2)}{T_2}\right] \text{Sin } \frac{2\pi t'}{T_2} - \cdots$$

$$+ \left[b_n \text{ Cos } \frac{2\pi(t_1-t_n)}{T_n} - a_n \text{ Sin } \frac{2\pi(t_1-t_n)}{T_n}\right] \text{Sin } \frac{2\pi t'}{T_n} \qquad (3)$$

where

$t' = t - t_1$ time scale on record 2 in seconds

$t_1 = \frac{\ell}{C_1}$; $t_2 = \frac{\ell}{C_2}$; $\cdots t_n = \frac{\ell}{C_n}$ time for each component to propagate the distance ℓ.

$C_1 = \frac{L_1}{T_1}$; $C_n = \frac{L_n}{T_n}$ - wave velocity of each component

L_1 = wave length of each component obtained from wave theory for known d and T_n*

d = still water depth ft.

Figure 18 shows a sketch of the time scale used with regard to $(t'+t_1-t_n)$. At position 2 the time of each component has a definite angle or argument $(\frac{2\pi t}{T_n})$ which for evaluation purpose must be separated into the time argument $(\frac{2\pi t'}{T_n})$ plus a phase angle $(\frac{2\pi(t_1-t_n)}{T_n})$. This later combination was used as

*Morison, J.R., "Analysis of Subsurface Pressure Records in Constant Depths and on Sloping [redacted], Series 3, Issue 336, Institute of Engineering Research, University of California, Berkeley, California, May 1952. and Wiegel, R.L., "Oscillatory Waves", Bulletin of Beach Erosion Board, Spec. Issue 1, 1948, Corps of Engineers

described in Equation 2. The resulting Equation 3 may be simplified mathematically, but such action may tend to complicate the final application which is relatively simple.

Several experiments were conducted in both the laboratory and the field. A few of these were analyzed with various degrees of success. In order to obtain good results the experiments and application of the method must follow or adhere to several rules as follows:

(i) The points of measurements and prediction must be in line and in the direction of wave propagation.

(ii) The wave system must be regular enough to have only one direction of propagation. The success of the method depends upon the waves behaving according to the linear wave theory.

(iii) At least three to six ordinates should be measured on the longest wave in order to obtain a satisfactory harmonic analysis. Since only the 48 point harmonic analysis scheme* was used this would limit the length of record analyzed, the greatest distance to the predicted point and the length of the predicted record.

There are of course other ways of doing this type of transformation but inherent to all is the limitation that the greater the distance propagated the greater is the length of measured record that must be analyzed. It might be better to say that this limitation is at least inherent to the linear wave theory.

Figure 19 shows the results of the laboratory study of wave transformation. Figure 19b shows the original measured surface wave system and its reconstruction by harmonic analysis which is a check on the accuracy of the wave components. Figures 19c, 19d, and 19e show the transformation of the wave after a travel distance of 10, 20 and 30 feet respectively together with the predicted or computed wave time history by the harmonic analysis method or Fourier Series analysis.

Figure 20 shows a field study where Figure 20b is the measured wave pressure and its reconstruction by harmonic analysis as a check on the wave components. Figure 20c shows the wave transformation after 204 feet of travel together with the predicted wave transformation

The results shown here are fairly good, but not all attempts were this accurate. Additional analyses of the accurately controlled field tests in progress will help to determine the validity of this method. One indication at this time is that the greater the travel distance the greater will be the error. This error appears in the phase relationship of the various components. Of course the effect of shoaling has not been taken into account. This problem is mainly whether or not all components can be separately transformed by shoaling and then recombined to give the actual transformed wave. This of course implies that the linear wave theory holds for shoaling waves, which is not true in general in relatively shallow water.

---

*Den Hartog, J.P. "Mechanical Vibrations", McGraw-Hill Book Co., Inc., New York and London, 1940

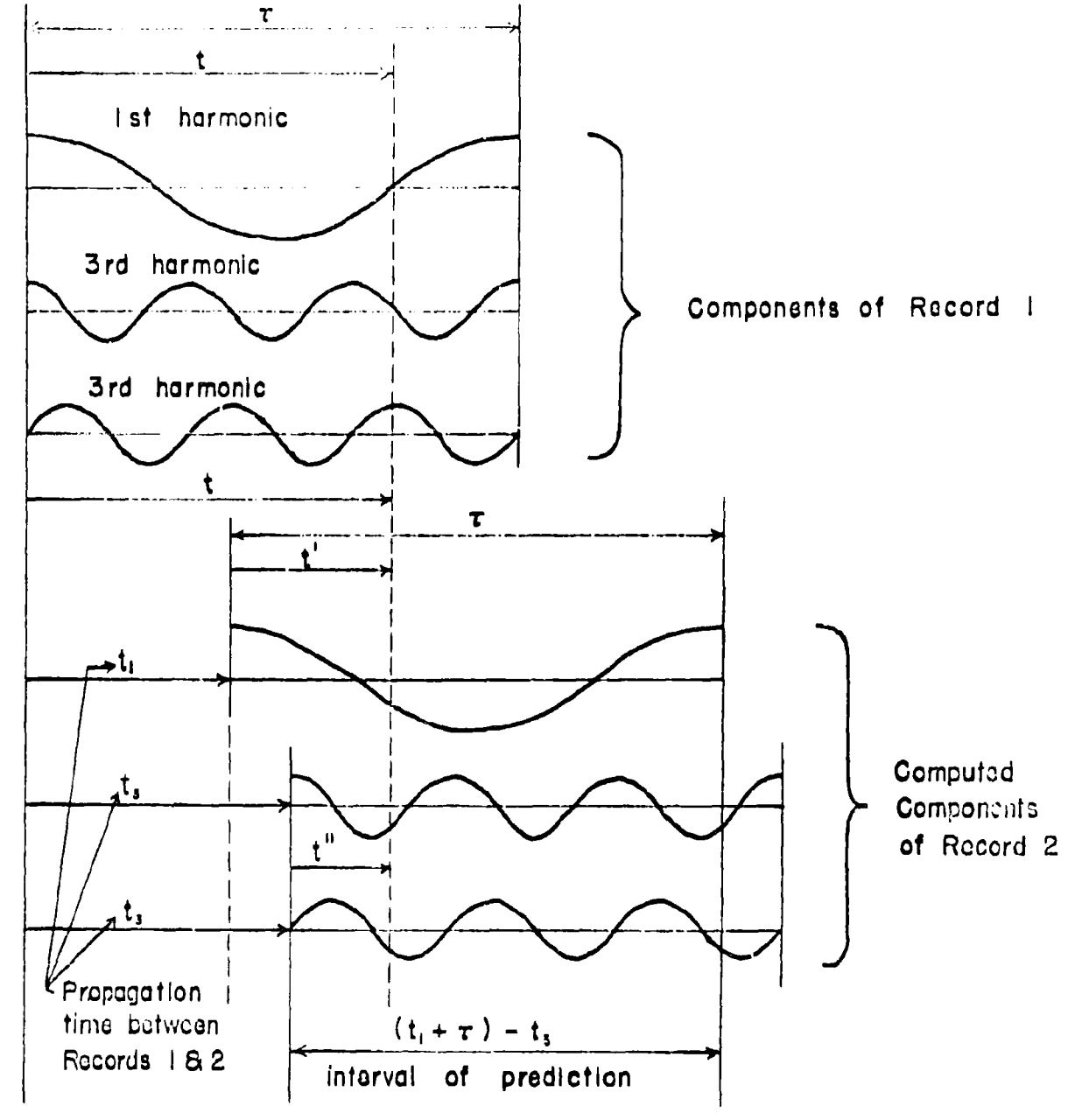

$$t = t_1 + t' \quad \text{or} \quad t' = t - t_1$$

$$t = t_3 + t'' = t_1 + t'$$

$$t'' = t' + t_1 - t_3$$

$$\therefore \; t^{n-1} = t' + t_1 - t_n$$

RESTRICTED
SECURITY INFORMATION

EXAMPLE OF TIME SCALES USED ON

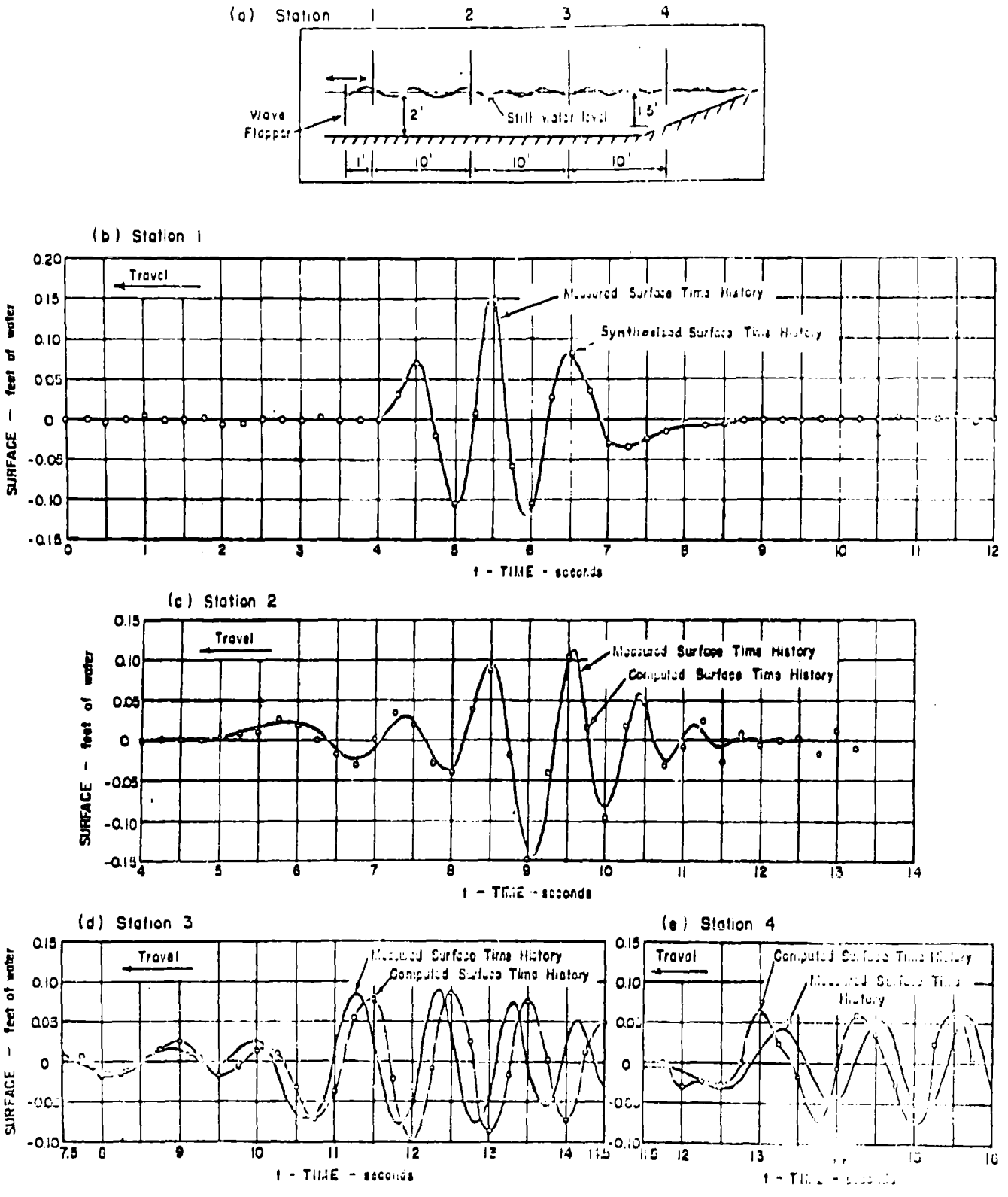

HYD-618I

MODEL STUDY OF WAVE TRANSFORMATION

RESTRICTED

FIGURE 10

(a)

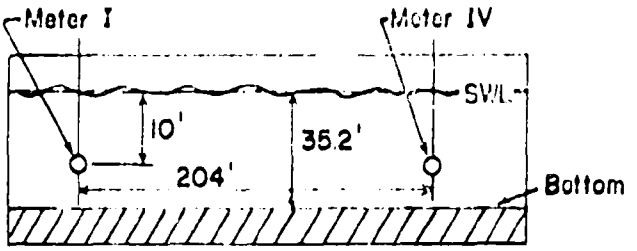

(b) Record I

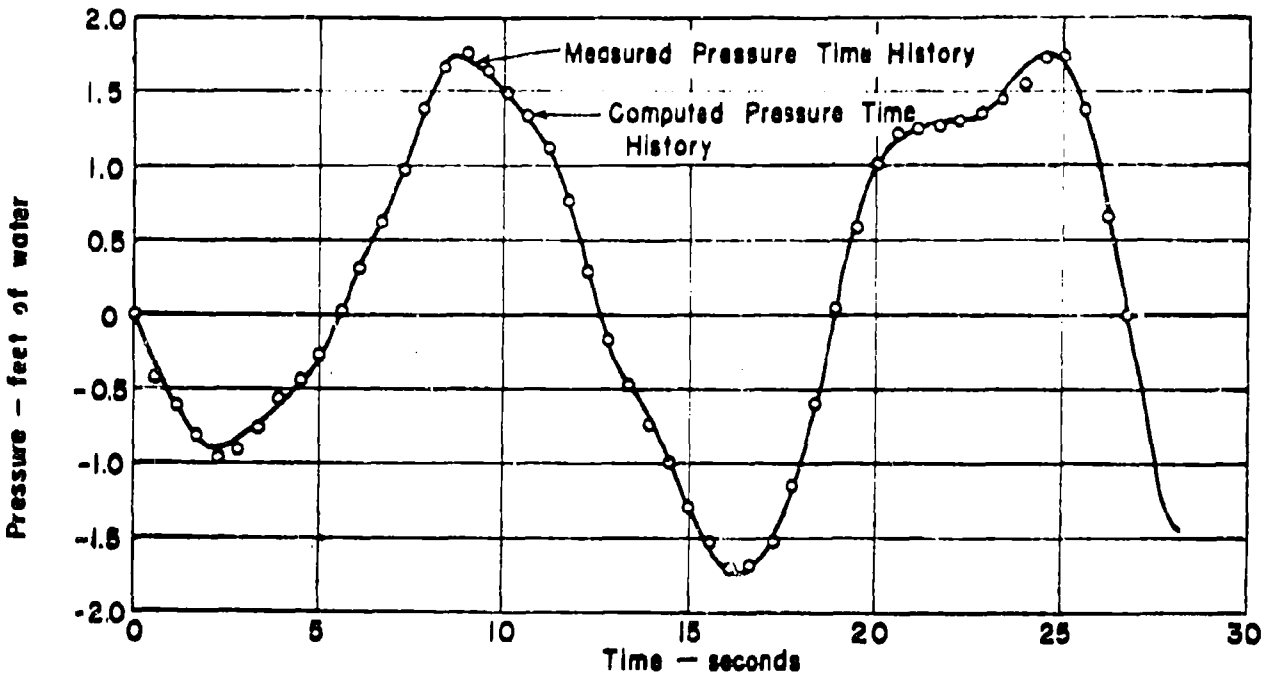

(c) Record IV

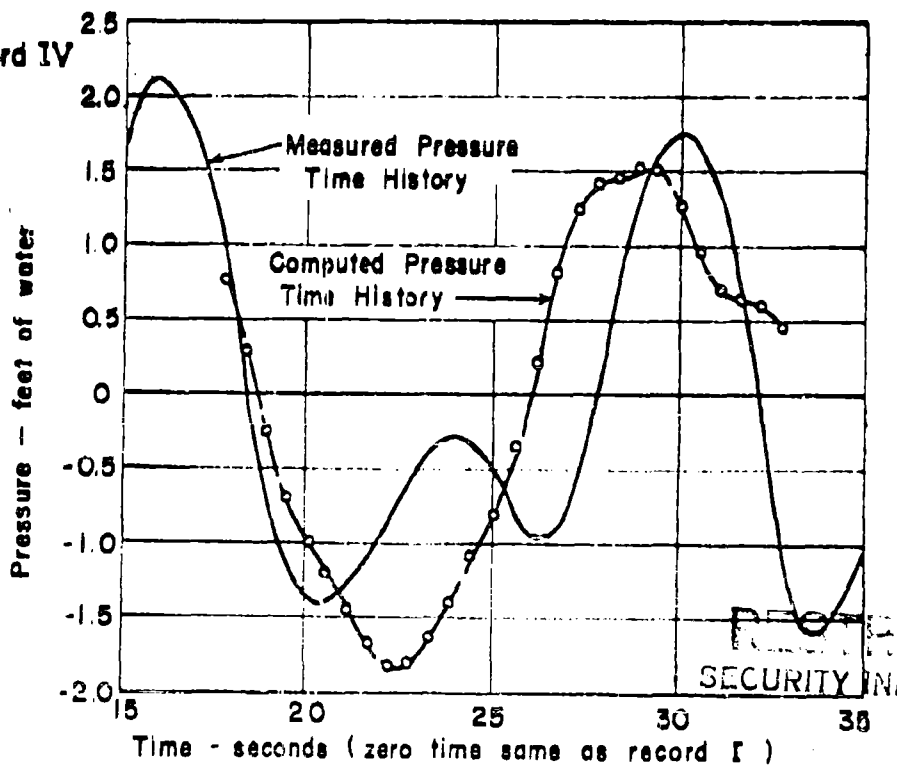

C. PREDICTABILITY OF WAVE TRANSFORMATION: LINEAR LEAST-SQUARES PREDICTION

Introduction

Within the problem of wave transformation there may arise the question of the degree of predictability inherent in the phenomenon apart from the theory employed for making the prediction or the means of carrying it out. If in particular a finite linear combination of discrete equally-spaced values of one observed variable is to be used to predict the other variable, the method of least squares may be employed to yield not only an optimum prediction kernel of this type but also a measure of the associated error of prediction. The preliminary studies described below were undertaken in order to show the degree of accuracy possible in predicting the transformation of waves.

The least squares method will rest on the interpretation of the two time-histories $f_t^{(1)}$, $f_t^{(2)}$ as the components of a two-dimensional discrete stationary random process. That is, they constitute a realization of a probabalistic system characterized (for present purposes) by three functions $\gamma^{(11)}$, $\gamma^{(12)}$, $\gamma^{(22)}$, each $\gamma^{(ij)}$ being the correlation function associated with $f^{(i)}$ and $f^{(j)}$. The direct computation of the least-squares prediction kernel described below depends on the previous knowledge of certain ordinates of the correlation functions and, while conceptually simple, its exact computation becomes tedious when the length of the kernel exceeds more than a few terms. The method, however, is applicable to any two time-history functions provided only that together they may be regarded as a random process of the kind described.

The required values of the correlation functions must be estimated from the observed sample time history, it being assumed that this sample represents a certain infinite (unobservable) time history.

The length, n, of the prediction kernel employed in the present studies was dictated by computational convenience. The time lag, l, between the time of the predicted ordinate $f_{t+l}^{(2)}$ and that of the latest ordinate $f_t^{(1)}$ used from the observed time history was determined so as to yield the best prediction. The prediction kernel then consists of a sequence of numbers $d_0, d_1, \ldots, d_{n-1}$ which, when applied to the observed time history, produce $\sum_{k=0}^{n-1} d_k f_{t-k}^{(1)}$ as the value predicted for $f_{t+l}^{(2)}$.

Linear Least-Squares Theory

It is assumed that suitable constants have been subtracted from the values of each of $f^{(1)}$ and $f^{(2)}$ so as to reduce the mean value of each to zero. Being given the prediction lag l and the kernel length n, the problem is to determine the sequence of real numbers $d_0, d_1, \ldots, d_{n-1}$, such that when the linear combination $\sum_{k=0}^{n-1} d_k f_{t-k}^{(1)}$ is formed for each given value of t, the mean, or expected, value of the squared error $\overline{\varepsilon^2} = \overline{\left[f_{t+l}^{(2)} - \sum_{k=0}^{n-1} d_k f_{t-k}^{(1)} \right]^2}$ is a minimum.

The necessary condition, $\frac{\partial \overline{\varepsilon^2}}{\partial d_j} = 0$, $j = 0, 1, \ldots, n-1$, for $\overline{\varepsilon^2} = \text{min.}$ can be

written $\sum_{k=o}^{n-1} d_k \overline{f^{(1)}_{t-j} f^{(1)}_{t-k}} - \overline{f^{(1)}_{t-j} f^{(2)}_{t+\ell}} = o$ for $j = o, 1, \ldots, n-1$, the bar denoting the (linear) mean-value operator. Introducing the correlation functions* $\gamma^{(11)}$, $\gamma^{(12)}$, this has the form $\sum_{k=o}^{n-1} d_k \gamma^{(11)}_{j-k} = \gamma^{(12)}_{j+\ell}$, $j=o, 1, \ldots n-1$.

The conditions on the d_k are thus those imposed by n simultaneous linear equations in n unknowns. Assuming these have a unique solution, the corresponding prediction kernel will yield the minimum least-squares error given by

$$\min \overline{\varepsilon^2} = \overline{\left[f^{(2)}_{t+\ell} - \sum_{k=o}^{n-1} d_k f^{(1)}_{t-k}\right]^2} = \gamma^{22}_o + \sum_{j=o}^{n-1} d_j \gamma^{(12)}_{j+\ell} - 2 \sum_{k=o}^{n-1} d_k \gamma^{(12)}_{k+\ell}$$

$$= \gamma^{(22)}_o - \sum_{j=o}^{n-1} d_j \gamma^{(12)}_{j+\ell}$$, using the condition on the d_k 's. A relative measure of the error of prediction suitable for many purposes is provided by the ratio of the root-mean-square error to the root-mean-square deviation of the observed time history from its average value. This ratio may be written

$$\left[1 - \frac{1}{\gamma_o^{(22)}} \cdot \sum_{j=o}^{n-1} d_j \gamma^{(12)}_{j+\ell}\right]^{\frac{1}{2}}$$

and may be computed from the values of the correlation functions alone. It is thus possible to determine what prediction lag and kernel length may best be used before any actual predictions are made.

Applications of the Theory

The finite linear least-squares prediction kernel was computed for three experimental sets of data, each corresponding to the transformation of wave systems between two points displaced horizontally in the general direction of wave propagation.

I. Laboratory Wave Channel - Here the wave-generating flapper was moved briefly and a short wave train of approximately one-second waves was started down the wave channel. At four stations, each one approximately ten feet from the preceding one, time histories of the surface elevation of the water were recorded for approximately 30 seconds. Predictions were made from the first station to each of the other three, as well as from the second to the third. Two representative examples are described below.

A. Station 4 from Station 1 - From measurements made every 0.1 second, values of $\gamma^{(11)}_o$, $\gamma^{(11)}_1$, ..., $\gamma^{(11)}_{\ell-1}$ and $\gamma^{(12)}_{105}$, $\gamma^{(12)}_{106}$, ..., $\gamma^{(12)}_{112}$ were estimated and used to compute an eight-term prediction kernel $d_o, d_1, \ldots, d_7$. Here $\ell = 105$, corresponding to 10.5 seconds, roughly ten times the wave period. The resulting prediction may be compared with the observed values at the second point in Figure 21a.

*The non-normalized correlation function $\gamma^{(ij)}_p$ for any two time history functions $f^{(i)}f^{(j)}$ is defined to be the average product $\overline{f^{(i)}_t f^{(j)}_{t+p}}$. It will be seen that, for $i=j$, and when the lag difference between subscripts is zero, the correlation function is merely the square of the r.m.s. value of the function $f^{(i)}$.

B. Station 3 from Station 2 - From measurements made every 0.1 second, values of $\gamma_0^{(11)}$, $\gamma_1^{(11)}$, ..., $\gamma_7^{(11)}$ and $\gamma_{21}^{(12)}$, $\gamma_{22}^{(12)}$, ..., $\gamma_{28}^{(12)}$ were estimated and used to compute an eight-term prediction kernel d_0, d_1, ..., d_7. Here $\ell = 21$, corresponding to 2.1 seconds, roughly twice the wave period. The resulting prediction may be compared with the observed time history at the second point in Figure 21b.

II. Ocean Waves, 28.5-foot Separation - Here the surface-elevation time history due to natural ocean-wave conditions was measured for a period of approximately five minutes at two stations separated by 28.5 feet. Predictions were made from the seaward station to the shoreward station. From measurements made every 0.5 second, values of $\gamma_0^{(11)}$, $\gamma_1^{(11)}$, $\gamma_2^{(11)}$, $\gamma_3^{(11)}$ and $\gamma_2^{(12)}$, $\gamma_3^{(12)}$, $\gamma_4^{(12)}$, $\gamma_5^{(12)}$ were estimated and used to compute a four-term kernel d_0, d_1, d_2, d_3. Here ℓ was taken as 2, corresponding to 1.0 second, roughly one-tenth of the mean wave period. The resulting prediction may be compared with the observed time history at the second point in Figure 22.

III. Ocean Waves, 205-foot Separation - Here the subsurface fluctuation time history due to natural wave conditions was measured for a period of 1000 seconds at two points separated by 205 feet and at depths of approximately 35 feet. Prediction was made from the seaward station to the shoreward station. From measurements made every 0.25 second values of $\gamma_0^{(11)}$, $\gamma_1^{(11)}$, $\gamma_2^{(11)}$, $\gamma_3^{(11)}$, and $\gamma_{17}^{(12)}$, $\gamma_{23}^{(12)}$, $\gamma_{29}^{(12)}$, $\gamma_{35}^{(12)}$ were estimated and used to compute the four-term prediction kernel d_0, d_1, d_2, d_3. Here $\ell = 17$, corresponding to 4.25 seconds, roughly one-third of the mean wave period. The resulting prediction may be compared with the observed time history at the second point in Figure 23a.

Further Use of Method

For the 28.5-foot ocean data an eight-term prediction kernel was also computed. The improvement in accuracy of this kernel over the previous four-term kernel did not appear to be significant enough to warrant the additional labor of computation. For the same data a prediction kernel of a different nature was computed, being so determined that the squared error of prediction was a minimum when averaged, not over the entire time history, but over only those times when the fluctuating surface deviated from its average value by at least $\sqrt{\pi/2}$ times its r.m.s. deviation from its mean value. Since $\sqrt{(\pi/2)\cdot\gamma_0^{11}}$ has been found in other studies to correspond to the height of an average wave measured from the level of its mean ordinate, when the total energy in the spectrum is $\gamma_0^{(22)}$, this kernel is designed to be accurate for higher-than-average waves. Although in principle such a kernel would be more suitable than the ordinary least-squares kernel if high waves are of especial importance, when applied to the present data there appeared to be little systematic difference in performance when the waves were high.

The 205-foot ocean wave data was subjected to a test of the assumption of temporal homogeneity, that is, that of its being stationary in time. In addition to the 1000-second time histories referred to above there was also measured at the same two points time histories of 60-seconds duration beginning approximately 30 minutes after the end of the earlier ones. No estimate was made of the correlation functions for these later time histories, but the prediction kernel computed for the earlier date was applied to the 60-second data. The results, shown in Figure 23b indicate that for purposes of linear least-square

prediction, the correlation functions have not changed significantly over a 30-minute interval.

The possibility of using the recently-developed Wave Ordinate Distribution Analyzer* for analog computation of estimates of the correlation function was also investigated by means of the 28.5-foot ocean-wave data. These estimates, based on the distribution of sums of the time-history functions with various time lags between them, would be relatively easy to compute. The results indicated that the estimates would be accurate enough to yield prediction kernels of the surface time history comparing favorably with those based on directly-computed values of $\gamma^{(11)}$ and $\gamma^{(12)}$.

Extensions of the Method

Modifications of the least-squares prediction methods described thus far may in certain cases be expected to yield somewhat better predictions. For example, one may carry out linear prediction of the time history at one point from observed time histories at two or more seaward points, a method which is perhaps suitable for non-uniform short-crested wave systems. An extension of the correlation function concept leads to non-linear prediction, a method which may be suitable for shallow-water prediction.

If the requirement to predict individual instantaneous time-history ordinates is relaxed, somewhat better prediction may be possible. Two alternative quantities whose prediction suggests itself are (1) the envelope of the time-history function and (2) the square of the ordinate integrated over a constant-length interval whose endpoints advance with time and whose duration is long compared with a wave period. The former would correspond to individual waves in the wave record while the latter would be proportional to a moving average of the energy over a fixed time interval.

Discussion of the Method

The advantages of the least-squares prediction methods for wave transformation are the relative shortness of the kernels required for accurate prediction, and their general applicability. They may be used on data taken under many conditions, whether capable of being dealt with by hydrodynamic theory or not. High accuracy, when obtainable, may be attributed to the fact that the method provides for each situation a solution which is tailor-made to it.

The chief disadvantages of the least-squares method are, of course, related to the specialness of the solution, in that special information — namely, values of the correlation functions — must be known before it can be used. This information, which is equivalent to a knowledge of certain features of the spectra of the two time histories involved, is required for each situation in which the method is to be applied. The labor of computing in each situation the correlation functions and the prediction kernel itself is an inconvenience which may be lessened by the utilization of analog computers for the purpose (e.g., the ordinate distribution analyzer mentioned above).

In those situations where it is known that hydrodynamic theory can predict the wave transformation that occurs between the two points, this knowledge may be used to determine any desired values of the correlation function $\gamma^{(12)}$, provided the correlation function $\gamma^{(11)}$ is known completely for the seaward point. In such a case a table may then be compiled, once and for all, showing

*Lund, W.W., "An Electronic Instrument for Statistical Analysis of Ocean Waves", University of California, Institute of Engineering Research, Technical Report, Series 3, Issue 343, September 1952.

the least-squares prediction kernel to be used for any given "input" spectrum, since the latter determines $\gamma^{(11)}$. Since this spectrum also determines those distances and times over which prediction will be most accurate, this information may likewise be tabled in such a case.

It remains to obtain a knowledge of the input spectrum (or correlation function), a problem which may be approached in various ways. In view of the results shown in Figure 23b an estimation of the correlation function based on data taken a short time (perhaps up to an hour) before the prediction was to be made would probably be sufficient. If the estimation of the correlation function were made even earlier, the change reflected in the values occurring later could undoubtedly be forecast to some extent from a knowledge of the past values of the function and from meteorological conditions. When adequate statistical data on ocean-wave spectra have been accumulated, sufficient regularity in their shape may be found to permit their characterization by a few parameters, and the rate of change of the latter with time may prove to be sufficiently slow to permit the prediction of spectra a short time in advance.

Summary Based on Preliminary Work

Examples presented above show that linear least-squares prediction of time-history ordinates can be applied to wave-transformation problems to yield moderately accurate predictions in the cases considered. When prediction over greater times and distances is attempted, the above-mentioned extensions of the method may be needed.

While the main purpose of the work described in this section on least-squares prediction was to investigate the degree of predictability inherent in phenomena of wave transformation, certain modifications of the techniques already employed have been mentioned in order to indicate that, should other methods of prediction prove inadequate, the least-squares method may perhaps be made serviceable. Much of the practical success of the method would seem to depend on the accumulation of knowledge of the form and frequency of occurrence of wave spectra under various conditions.

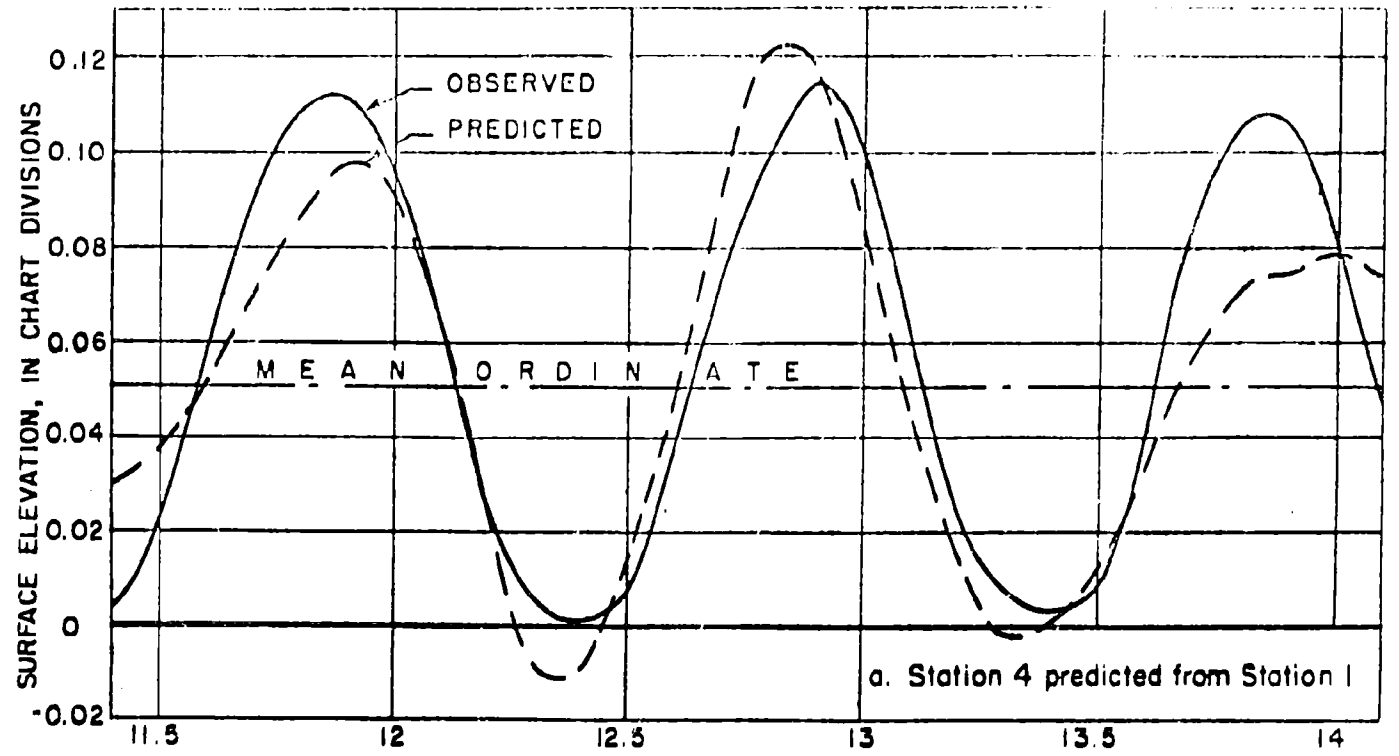

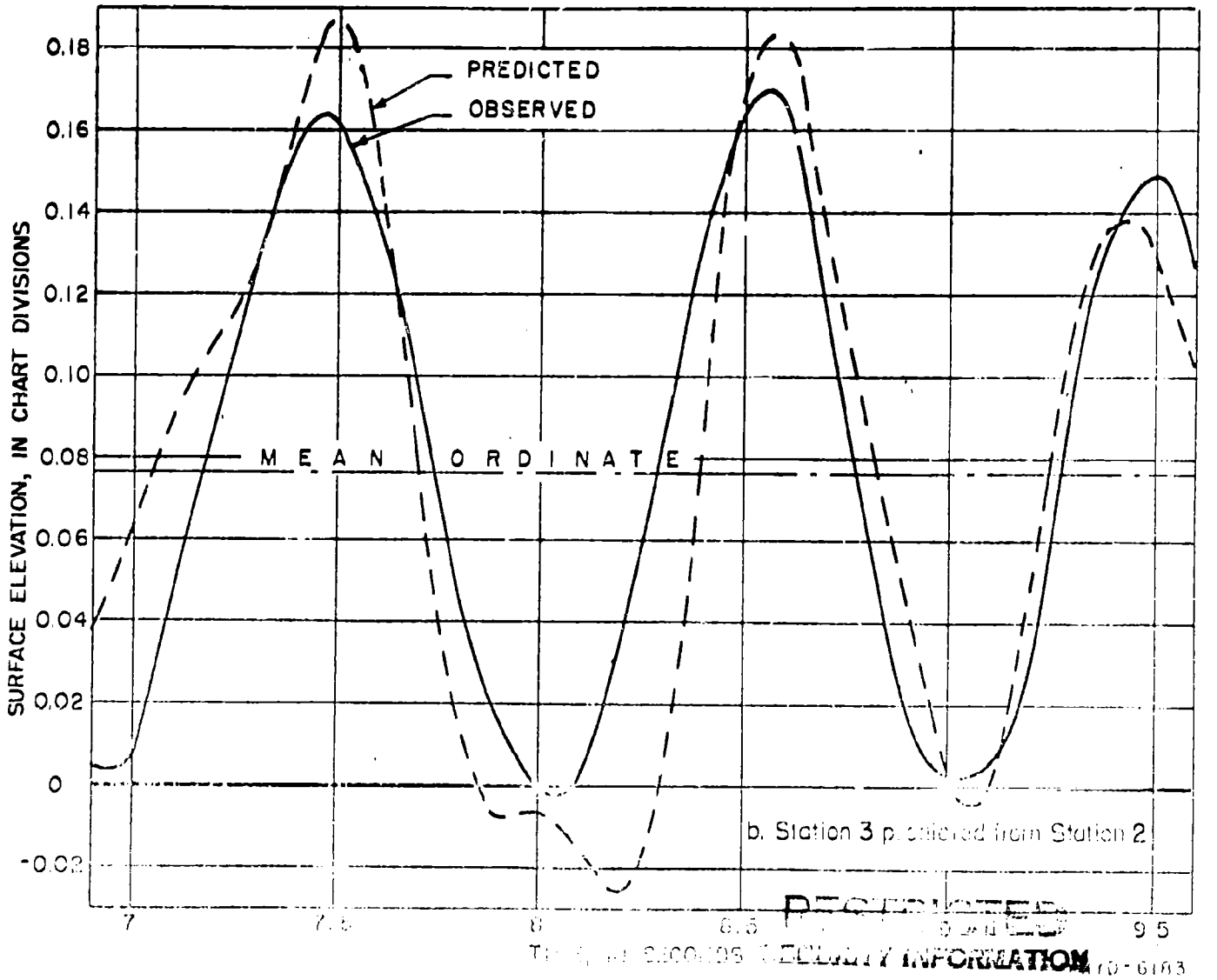

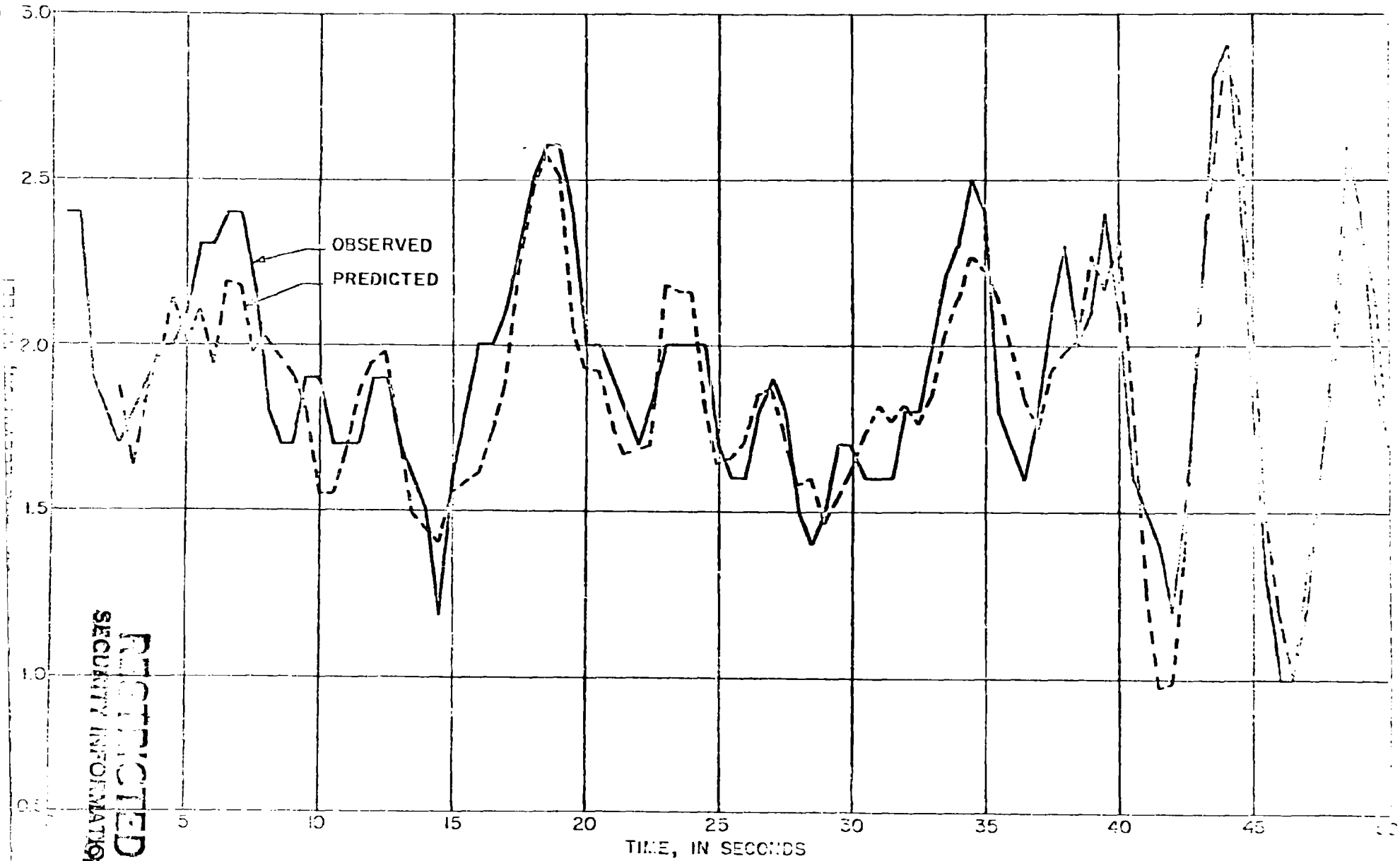

OCEAN WAVE PREDICTION OVER 200-FOOT DISTANCE, LEAST SQUARES METHOD

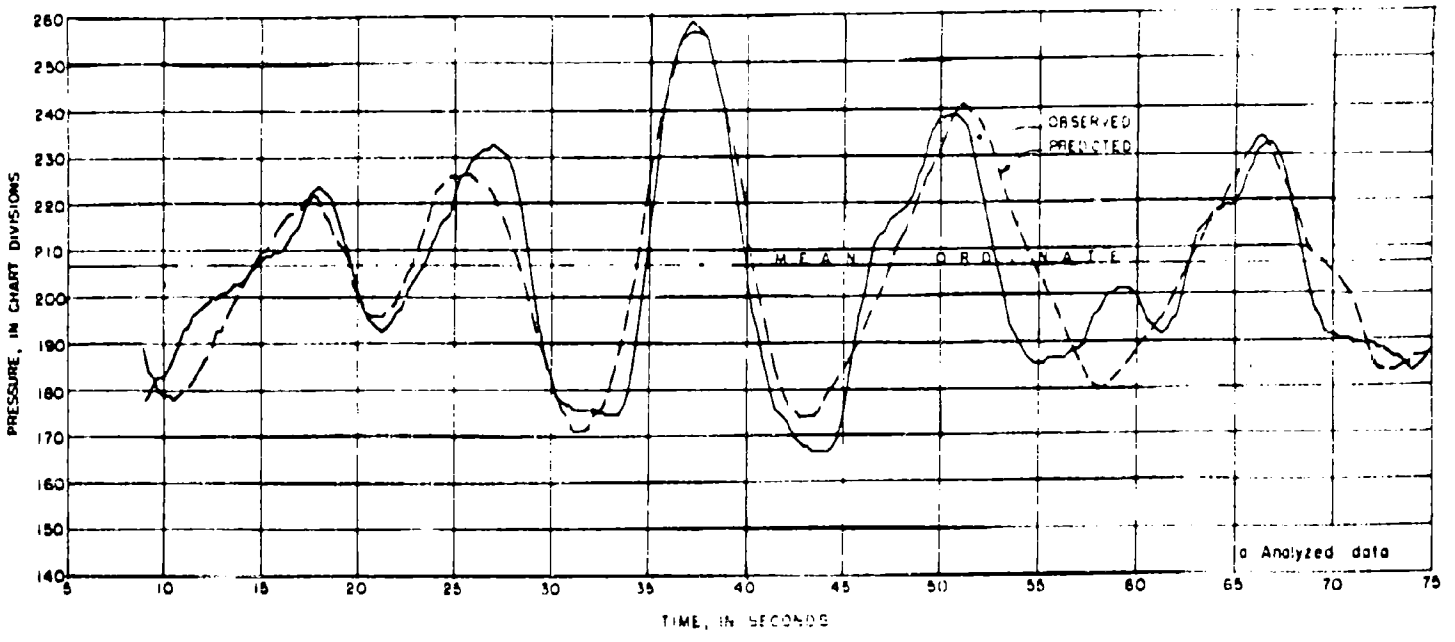

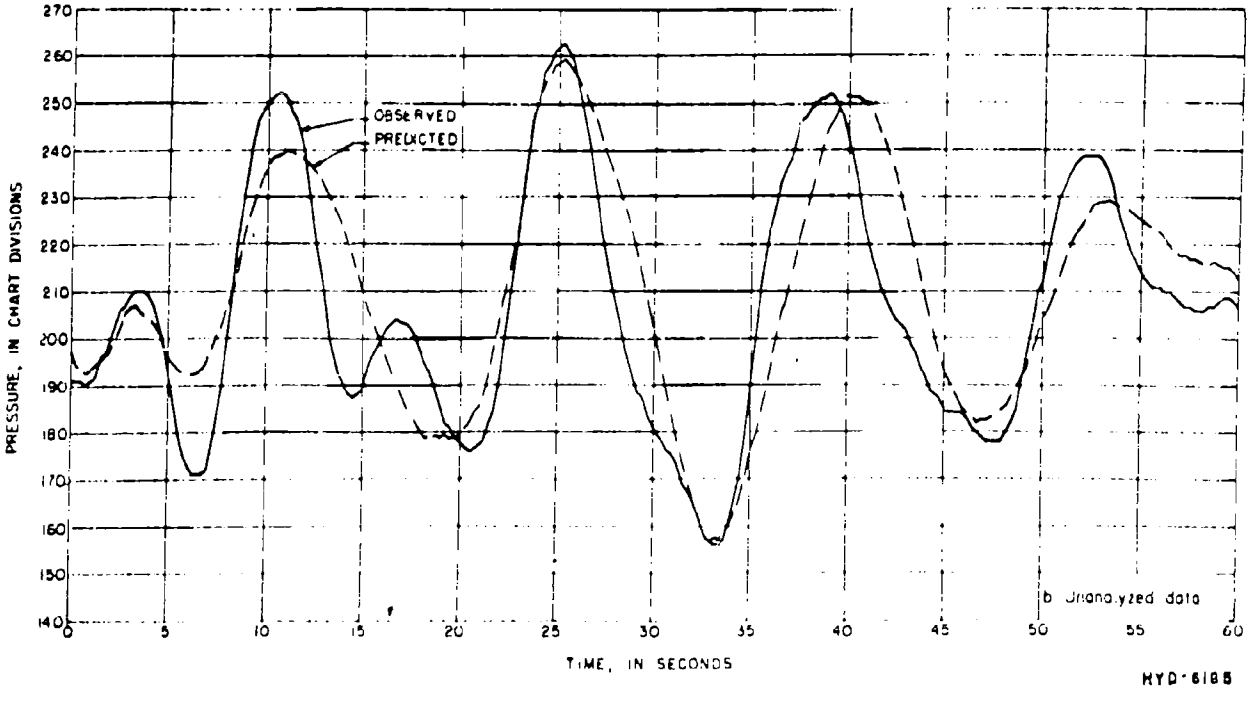

OCEAN WAVE PREDICTION OVER 204-FOOT DISTANCE, LEAST SQUARE METHOD

FIGURE 23

DISTRIBUTION LIST

Technical Reports on Project NR256-001 (Contract Nonr-222(15)

1 Chief of Naval Research
Navy Department
Washington 25, D.C.
Attention: Code 465

3 Chief of Naval Research
Navy Department
Washington 25, D.C.
Attention: Code 416

1 Naval Research Laboratory
Technical Services
Washington 25, D.C.

2 Director
U.S. Naval Electronics Laboratory
San Diego 52, California
Attention: Codes 550, 552

1 Chief, Bureau of Yards & Docks
Navy Department
Washington 25, D.C.

1 Commanding General
Research & Development Division
Department of the Army
Washington 25, D.C.

1 Commanding Officer
Cambridge Field Station
230 Albany Street
Cambridge 39, Massachusetts
Attention: CRHSL

1 Chief of Naval Research
Navy Department
Washington 25, D.C.
Attention: Code 486

2 Asst. Naval Attache for Research
American Embassy
Navy 100
Fleet Post Office, New York

8 U.S. Navy Hydrographic Office
Washington 25, D.C.
Attention: Division of Oceanography

2 Chief, Bureau of Ships
Navy Department
Washington 25, D.C.
Attention: Code 847

1 Commander
Naval Ordnance Laboratory
White Oak, Silver Spring 19,
Maryland

1 Commanding General
Research & Development Division
Department of the Air Force
Washington 25, D.C.

1 Research & Development Board
National Military Establishment
Washington 25, D.C.
Attention: Committee on Geophysics
and Geography

1 Director
Office of Naval Research
150 Causeway Street
Boston, Massachusetts

1 Director
Office of Naval Research
844 North Rush Street
Chicago 11, Illinois

1 Director
Office of Naval Research
1000 Geary Street
San Francisco 9, California

1 Commandant (OAO)
U.S. Coast Guard
Washington 25, D.C.

1 U.S.Army Beach Erosion Board
5201 Little Falls Road, N.W.
Washington 25, D.C.

1 Director
Chesapeake Bay Institute
Box 426A RFD#2
Annapolis, Maryland

1 Director
Narragansett Marine Laboratory
Kingston, Rhode Island

1 Head, Department of Oceanography
University of Washington
Seattle, Washington

1 Director
Office of Naval Research
346 Broadway
New York 13, New York

1 Director
Office of Naval Research
1030 E. Green Street
Pasadena 1, California

1 Director
U.S. Coast and Geodetic Survey
Department of Commerce
Washington 25, D.C.

1 Department of Engineering
University of California
Berkeley, California

2 Director
Woods Hole Oceanographic Institution
Woods Hole, Massachusetts

1 Director
Marine Laboratory
University of Miami
Coral Gables, Florida

2 Director
Scripps Institution of Oceanography
La Jolla, California

1 Head, Department of Oceanography
Texas A & M College
College Station, Texas

1 Commander
Amphibious Training Command
U.S. Pacific Fleet
San Diego 32, California